THESIS FOR THE DEGREE OF DOCTOR OF PHILOSOPHY

Application of high-frequency mechanical impact treatment for fatigue strength improvement of new and existing bridges

HASSAN AL-KARAWI

Department of Architecture and Civil Engineering
Division of Structural Engineering
Lightweight Structures
CHALMERS UNIVERSITY OF TECHNOLOGY

Gothenburg, Sweden 2023

Application of high-frequency mechanical impact treatment for fatigue strength improvement of new existing bridges
HASSAN AL-KARAWI
ISBN 978-91-7905-797-8

Doktorsavhandlingar vid Chalmers tekniska högskola
Ny serie nr 5263
ISSN 0346-718X

Department of Architecture and Civil Engineering
Chalmers University of Technology
SE-412 96 Gothenburg
Sweden
Telephone + 46 (0)31-772 1000

Cover:
[Micrographs of welded details before and after HFMI treatment, centered by a photo showing the HFMI device are shown in the foreground. In the background, a photograph of two examples of steel bridges located in Gothenburg is shown. Source: Göteborgs Stad]

[Chalmers Reproservice]
Gothenburg, Sweden 2023

To my late friend, Ala'a

1996-2016

CHALMERS

Erratum to "Application of high-frequency mechanical impact treatment for fatigue strength improvement of new and existing bridges"

Hassan Al-Karawi

This is a corrigendum and clarification on behalf of the author for the mistakes in the thesis and the appended papers. The corrections are given in a table format which lists both the mistakes and the corrections.

Where to find	Written as	Should be
Page 15, Line 15 & Page 16, Line 1	… plane strain…	… plane stress …
Page 17, Lines 16-18 **Paper 3, Figure 6 & Left lines 26-27** **Paper 3, Page 6, Right lines 8-9** **Paper3, Page 7, Left line 1**	… stress range …	… stress amplitude…
Page 17, Figure 2.12	Elements to model TIG transisition.	Elements to model TIG transition.
Page 18, Equation 2.4 & Figure 2.13 **Paper 3, Equation 4**	$\Delta\epsilon$	$\Delta\epsilon$ / 2
Page 23, Line 22	…the indeuced compressive…	… the induced compressive
Page 28, Line 26	… is not expected to affect …	… is not expected to be affected by …
Page 34, Equation 3.10 **Paper 7, Equation 4**	$-(x-u-\ln\lambda)$	$-(x-u-m\times\ln(\lambda))$
Page 44, Line 36	… in the last decade.	… in the last decades.
Paper 3, Figure 9	For the blue curve, f (0) = -172 MPa	For the blue curve, f (0) = -111 MPa
Paper 4, Page 1, Right line 15-16	, while the latter case resembles…	, while the latter case better resembles …
Paper 4, Page 3, Left line 10-11	Failure occurs …	For AW specimens, failure occurs …
Paper 4, Table 1, line 3	HFMI, corrosion, then fatigue testing	corrosion, HFMI, then fatigue testing
Paper 4, Table 1, line 10	…the fatigue testing	… then fatigue testing.
Paper 4, Table 1, lines 5 & 8	Test type: Immersion	Test type: Salt spray
Paper 4, Table 1, lines 6 & 9	Test type: Salt Spray	Test type: Immersion
Paper 4, Table 1, lines 8 & 9	Thickness: 15 mm	Thickness: 25 mm
Paper 4, Figure 5	Wrong caption	Concentration effect on the efficiency of HFMI treatment
Paper 4, Table 2	… of the transverse attachment …	of the studied details …
Paper 6, Page 1, Lines 22-24	Wrong lines	Should be removed
Paper 6, Page 1, Line 35	There-fore,	Therefore,
Paper 6, Page 4, Line 5	… is shown in Fig-ure 4.	… is shown in Figure 4.
Paper 6, Page 9, Line 16	… is that the av-erage R-ratio …	… is that the average R-ratio …
Paper 6, Page 9, Line 18	… larger than the equiv-alent stress…	… larger than the equivalent stress …
Paper 6, Equation 16 (top)	$\geq$	$\leq$
Paper 6, Page 13, Line 27	… accumu-lation methods …	…accumulation methods…

Application of high-frequency mechanical impact treatment for fatigue strength improvement of new and existing bridges

HASSAN AL-KARAWI
Department of Architecture and Civil Engineering
Division of Structural Engineering, Lightweight Structures
Chalmers University of Technology

ABSTRACT
This thesis investigates the application of High-Frequency Mechanical Impact (HFMI) treatment for fatigue strength improvement of weldments in existing and new bridges. In the former case, the welds have already been subjected to fatigue loading and accumulated damage before treatment. A fatigue testing program is set up, comprising welded specimens subjected to fatigue loading before HFMI treatment to investigate the efficiency of HFMI treatment on existing structures. Moreover, additional fatigue test results are collected from the literature and analyzed. HFMI treatment is found to be very efficient in extending the fatigue lives of existing structures regardless of the accumulated fatigue damage prior to treatment, given that any surface cracks, if exist, have not grown more than 2.25 mm in depth. For practical applications, HFMI treatment is only recommended if the critical details are verified to be free of any surface cracks.

Remelting the surface with a tungsten electrode before HFMI treatment is another solution which has rarely been studied on existing structures. Therefore, several experimental investigations are conducted including fatigue testing, measurement of residual stress, hardness testing and scanning the welds topography to study the effect of combining these two post-weld treatment techniques. The combined treatment is found to be efficient as it induces higher and deeper compressive residual stress and local hardening. These aspects are all considered in numerical simulations conducted to investigate the fatigue behaviour of new and existing weldments treated using this combination. The results verify the superiority of the combined treatment to both individual treatments (TIG & HFMI). Nonetheless, because of the complexity associated with TIG remelting, the combination is only suggested for existing structures containing shallow fatigue cracks which can be fused by tungsten electrode.

One major hindrance to applying HFMI treatment on weldments in steel bridges is the lack of design rules and recommendations such as consideration of stress ratio (mean stress) and overloads. Therefore, a correction factor (called λ_{HFMI}) to account for the mean stress effect is derived. This factor is used to magnify the design stress range for fatigue verification of HFMI-treated welded details existing in road and railway bridges. λ_{HFMI} is calibrated using measured traffic data that includes millions of vehicles and hundreds of trains. In addition, the characteristic load combination associated with the serviceability limit state is found to be the most appropriate for verifying the maximum stresses in road bridges. Based on the work conducted in this thesis, a complete methodology is proposed for the design and assessment of HFMI-treated welded details in new and existing steel bridges.

Finally, the effect of corrosion on the performance of HFMI-treated weldments is studied by analysing collected test results. Despite the observed reduction in fatigue endurance of HFMI-treated details due to the removal of top layers improved by residual stresses, the obtained fatigue lives are still longer than the design lives assigned for new welded details even in extreme corrosion conditions. However, corrosion protection and removal of sharp HFMI groove edges via light grinding are still necessary to reduce the susceptibility of weldments to corrosion.

Keywords: HFMI, Life extension, Post-weld treatment, Crack detection, Finite element, Variable amplitude, Bridges, Steel, Corrosion, Fatigue

Preface

The work presented in this thesis was carried out in the time between September 2018 to January 2023 at the research group of Lightweight Structures - Chalmers University of Technology. This research was conducted as part of three research projects funded by the Swedish Transportation Administration and the Swedish research agency Vinnova.

First, I would like to direct my gratitude to my supervisor Prof. Mohammad Al-Emrani for his support and guidance throughout the entire period of my PhD studies. Dr Poja Shams-Hakimi, Dr Franz von Bock, Dr Asma Manai, Dr. Reza Haghani and Joakim Hedegård , for their support in this project, is deeply appreciated. I would like to thank you all for supporting me in this project.

I also want to thank my parents, wife and siblings for all their love and support. I wish you all the best in life. You may know that engineering is an important part of my life, but you all are the real treasure I do have.

HASSAN AL-KARAWI

List of publications

The thesis is based on the following publications:

1. **Al-Karawi**, H, and Von Bock und Polach, F and Al-Emrani, M, 2020. Fatigue crack repair in welded structures via tungsten inert gas remelting and high-frequency mechanical impact. Journal of Constructional Steel Research, 172, p.106200.

   Summary of the paper This paper investigates the efficiency of TIG-remelting followed by HFMI in fatigue life extension of existing cracked welded structures. Fatigue tests, and other auxiliary experimental investigations were carried out to measure the residual stress, hardness and local geometry. The treated weldment is found to be stronger than the base metal. Besides, the combined treatment causes an improvement in the local geometry due to TIG remelting , and compressive residual stress and local hardness due to HFMI treatment.

   Author's contribution The author of this thesis is the corresponding author who wrote the different sections in this paper. The author composed the literature study, participated in planning and execution of the several experimental investigations made in this paper including the fatigue testing and other auxiliary investigations. The author conducted also the fatigue life calculations made in this paper.

2. **Al-Karawi**, H and von Bock und Polach, F and Al-Emrani, M, 2021. Fatigue life extension of existing welded structures via High Frequency Mechanical Impact treatment. Engineering structures 239, p.112234.

   Summary of the paper This paper investigates the efficiency of HFMI treatment in extending the fatigue life of existing structures containing fatigue cracks through fatigue testing. The capability of HFMI treatment in enhancing the fatigue lives is demonstrated. However, the efficiency decreases as the crack size increases. Nonetheless, a literature study showed that all fatigue test results on transverse attachment give fatigue lives longer than the design lives proposed by the IIW recommendations. Besides, it was shown that the depth of induced compression by HFMI treatment reaches 1.5-2.0 mm in most cases.

   Author's contribution The corresponding author is responsible for conceptualization, methodology, investigation, data curation, formal analysis, validation and Visualization and original drafting.

3. **Al-Karawi**, H, 2021. Fatigue life estimation of welded structures enhanced by combined thermo-mechanical treatment methods. Journal of Constructional Steel Research. 187, P.106961

   Summary of the paper This paper presents finite element simulations of thermo-mechanical post-weld treatments using TIG remelting followed by HFMI treatment. In the simulations, the change in residual stress is evaluated numerically and incorporated in the analysis while hardness and local geometry were measured and included explicitly. The fatigue lives were then evaluated via fatigue damage modelling and finite element deletion. The combined treatment is found to give longer fatigue life than TIG or HFMI treatment when they are applied alone.

   Author contribution The corresponding author is the sole author of the paper.

4. **Al-Karawi, H**. "Corrosion Effect on the Efficiency of High-Frequency Mechanical Impact Treatment in Enhancing Fatigue Strength of Welded Steel Structures." Journal of Materials Engineering and Performance (2022): 1-8.

Summary of the paper This paper investigates the effect of steel corrosion on the efficiency of HFMI treatment in enhancing fatigue resistance. More than 150 fatigue test results on corroded and HFMI-treated welded details are collected from several research articles and analyzed for both transverse welded attachment and butt-welded details. The efficiency of HFMI treatment decreases in corroded details as the corrosion level increases. However, HFMI treatment is found to have a high potential in prolonging the fatigue life, even in circumstances of an extremely corrosive environment.

Author contribution The corresponding author is the sole author of the paper.

5. **Al-Karawi**, H and Hakimi, PS, Al-Emrani, m, 2022. Mean Stress Effect in High-Frequency Mechanical Impact (HFMI)-Treated Steel Road Bridges, Buildings.

   Summary of the paper This paper validates a previously proposed design method to consider the mean stresses in HFMI treated road bridges via traffic measurements in Sweden and the Netherlands. The possibility of considering the mean stress via Eurocode's fatigue load models was also investigated. The design method which includes the self-weight and the variation in R-ratio due to traffic load is validated for use in both countries. Besides, the mean stress effect could not be accurately predicted using FLM3 or FLM4 load models.

   Author's contribution The corresponding author conducted the literature study, the analysis, the validation and the study on different load models. Besides, the author also conducted the fatigue verification presented in the paper using λ-coefficients and damage accumulation methods.

6. **Al-Karawi**, H and Shams-Hakimi, P and Petursson, H and Al-Emrani, M. 2022 Mean stress effect in High-Frequency Mechanical Impact (HFMI) treated welded steel railway bridges. Submitted to Steel Construction.

   Summary of the paper This paper investigates the mean stress effect in railway steel bridges enhanced via HFMI treatment. Traffic data are collected, analyzed and used to study the mean stress effect. Thereafter, a factor to include the stress ratio (or mean stress) effect is proposed to be used in magnifying the design stress range in fatigue verification. Moreover, the mean stress could not be predicted using most of the Eurocode traffic load models such as LM71, SW and train mixes.

   Author's contribution The corresponding author conducted the literature study, the analysis, the validation and the study on different load models. Besides, the author also conducted the fatigue verification presented in the paper using λ-coefficients and damage accumulation methods.

7. **Al-Karawi**, H and Leander, J and Al-Emrani, M. 2023, Verification of the Maximum Stresses in Enhanced Welded Details via High-Frequency Mechanical Impact in Road Bridges, Buildings.

   Summary of the paper The maximum service stresses that can be allowed on HFMI-treated joints should be controlled to avoid the relaxation of the induced compressive residual stress. Therefore, this paper aims at providing a base for verifying the maximum stress in steel road bridges via statistical analysis of recorded traffic. The paper compares the measured maximum traffic loads to those generated by load models considering different combinations. It is found that the characteristic load combination is the best-studied alternative to verify the maximum stress in road bridges.

   Author's contribution The corresponding author performed the statistical analysis, and written the original draft of the manuscript.

Additional contributions from the author

1. **Al-Karawi, H**., and Al-Emrani, M., 2021. The efficiency of HFMI-treatment and TIG-remelting of existing welded structures. Steel Construction.

2. **Al-Karawi, H** and von Bock und Polach, F and Al-Emrani, M, 2021. Crack detection via strain measurements in fatigue testing. Strain, p.e12384.

3. Hakimi, PS and Carlsson, F and Al-Emrani, M and **Al-Karawi, H**, 2021. Assessment of in-service stresses in steel bridges for high-frequency mechanical impact applications. Engineering structures. 241, P.112498

4. **Al-Karawi, H**, 2021. Material and residual stress improvement in S355 welded structural steel by mechanical and thermal post-weld treatment methods. Steel Construction

5. **Al-Karawi, H**, 2022, Literature review on crack retrofitting in steel by Tungsten Inert Gas remelting Ships and Offshore Structures, Ships and Offshore Structures.

6. Hakimi, PS and **Al-Karawi, H** and Al-Emrani, M, 2022. High cycle variable amplitude fatigue experiments and a design framework for bridge welds treated by high-frequency mechanical impact, Steel Construction

7. **Al-Karawi, H** and Al-Emrani, M and and Hedegård, J. "Crack behavior after high frequency mechanical impact treatment in welded S355 structural steel." in the proceeding of the tenth International Conference on Bridge Maintenance, Safety and Management, Sapporo, Japan (2021)

8. **Al-Karawi, H** and Manai, A and Al-Emrani, M and von Bock und Polach, F and Friedrich, N and Hedegård, J. "Fatigue crack repair by TIG-remelting." in the proceeding of the tenth International Conference on Bridge Maintenance, Safety and Management, Sapporo, Japan (2021).

9. **Al-Karawi**, H, Al-Emrani, M and Haghani, R. " Fatigue life estimation of treated welded attachments via High Frequency Mechanical Impact treatment (HFMI-treatment." Modern Trends in Research on Steel, Aluminum and Composite Structures, Poznań, Poland (2021).

10. **Al-Karawi**, H and Al-Emrani, M. Fatigue life extension of welded steel structures by High Frequency Mechanical Impact (HFMI)." proceeding of the Eurosteel , Sheffield, England (2021).

Contents

1 Introduction

1.1 Background

After world war II, thousands of bridges were built in order to meet the needs for road and railway networks. Therefore, traffic authorities in Europe are dealing today with many bridges which are structurally deficient, functionally obsolete or in need of repair and upgrading. The collected data from 17 railway administrations show that more than two-thirds of the railway bridges in Europe are older than 50 years, and half of them are even older than 100 years [1]. In France, more than 50 % of 20,000 bridges need to be repaired, while more than 20 % of the bridges are structurally deficient. In Hungary, an urgent repair is needed for more than half of the main and secondary bridges [2]. In general, there are two solutions to handle ageing bridges: they should either be replaced, and new bridges are to be constructed, or the bridges should be, alternatively, upgraded and any existing damage should be repaired.

Out of the 161 failed metallic bridges studied in [3], fatigue and fracture are the most critical failure modes that constitute more than 45% of the total studied pole. Therefore, the fatigue limit state (FLS) should be taken into consideration in the design of steel and steel-concrete composite bridges. Fatigue is defined as a progressive localized permanent damage which occurs in metallic connections and evolves when the structure is subjected to repeated loading even if the generated stress ranges are lower than the yield strength of the material [4]. This damage accumulates and causes crack formation which propagates upon more load cycles and causes failure in the structure. Considering the traffic load which generates millions of cycles acting on the structural components, fatigue can be, in many cases, the governing criterion in the design of steel bridges as it may limit the design load to a lesser value than both the ultimate and the service limit states [5].

When the welding was introduced in Europe as an alternative joining method to riveting prior to world war II, several welded pedestrian truss bridges were constructed. Welding was then used in different types of metallic bridges such as road and railway bridges. Nowadays, welding is by far the most predominant joining method used in steel bridges and other industries. However, fatigue failures have been observed in many bridges and, in some cases, the failure was brittle and sudden [3]. This drew the engineers' and researchers' attention to the phenomenon of fatigue in welded connections. In the 1960s, the American Association of State Highway and Transportation officials (AASHTO) introduced fatigue design provision [6]. The stress range concept and the detail categories were then introduced in the 1970s [7]. Two decades later, a whole chapter was devoted to the fatigue design of steel structures in the Eurocode [8]. At the beginning of the 21^{st} century, recommendations for fatigue design of welded structures were released by the International Institute of Welding (IIW) [9].

Despite being the most predominant joining method, welding usually induces unfavourable tensile residual stresses in the heat-affected zone. Furthermore, welding introduces geometrical stress concentration due to the disturbance of the stress flow in the metal because of the geometrical changes such as welded attachment. Moreover, weld defects such as undercuts or spatter can be generated after welding. Because of these defects, the number of cycles that causes crack initiation at the weld toe is relatively shorter than in plain members. Fatigue cracks, in most cases, initiate from the weld toe and propagate through the base metal or, in some cases, from the weld root and propagate through the weld body [10].

Because of the aforementioned challenges associated with the welding process, several weld-strengthening methods have been studied, developed and investigated in numerous test programs. The choice of the method is determined by a variety of factors including the circumstance of fatigue cracking, the availability of the required skills and operators, and the size of the crack if one exists. Drilling a hole at the tip of the fatigue crack is a practice that reduces the potential of crack propagation. This practice is called hole

drilling. The hole should have enough size to arrest the crack [11]. Besides, crack inspection is required to designate the crack tip location, which might be difficult as the crack tip is usually faint. In addition, the hole can be plugged with a tightened bolt to introduce compression forces and cause further crack retardation [12]. However, the crack, in this case, should be large, usually through-thickness crack.

Re-welding is another technique that can be used for the repair of long fatigue cracks [13]. The damaged material should be first removed by grinding, and then it should be filled with weld material. Thus, the whole cracked region is replaced by new welds. In many cases, the new weld exhibits the same fatigue strength as the original uncracked weld [14]. However, this method has deleterious effects on the mechanical properties of the material. Besides, there is a risk of smearing the crack during material removal. In addition, re-welding may also induce undesired tensile residual stress and distortions due to the extreme heat input. Nevertheless, these effects can be counteracted by using mechanical impact to introduce compressive residual stress.

Another strategy to reduce the susceptibility to fatigue cracking is to reduce the nominal stresses in the structural members. This can be done by increasing the plate area or by attaching a cover plate via welding or bolting [15]. However, this introduces a source of stress concentration and negatively affects fatigue strength. Furthermore, this method requires good accessibility to the crack position and requires traffic to shut down temporarily. It also contributes to increasing the in-service mean stresses due to the self-weight increase.

All the aforementioned methods (crack-arrest hole, re-welding, and splicing) are applicable for fatigue enhancement of structures containing relatively long fatigue cracks [16]. However, this is not often the case in most existing bridges where the weldments contain no or relatively short cracks. Therefore, there is another family of methods that have a more local effect such as grinding, impact treatment and remelting. These methods are specified in the IIW recommendations on post-weld improvement of steel and aluminium structures [17]. They are mainly intended to be used for fatigue strength improvement in new structures. However, they might have the potential, in some circumstances, to be used for fatigue life extension of existing structures. These methods can be classified into two categories based on their primary effect: stress concentration reducers and residual stress improvers. In the former one, the aim is to reduce or remove the local stress concentration by smoothing the transition of the weld toe by either fusion using a tungsten electrode or grinding using a burr disk [4].

In comparison with Tungsten Inert Gas (TIG)-remelting, grinding is a slower process, especially when applied to hard material, which also causes wear in the disk used for grinding. Moreover, more effort is needed from the operator for grinding when compared to remelting [18]. Furthermore, the fatigue strength of TIG-remelted details is found to be higher than these of ground details [18, 19]. This technique aims at creating a weld pool, remelting the vicinity of the weld toe, removing any existing defect, providing a transition between the weld and the base material, and thereby, reducing the local stress concentration [20]. Moreover, it influences the microstructure of the material and changes the residual stress level at the weld toe. The depth of fusion and the radius of the new weld toe can be optimised by controlling the heat input, which is dependent on the remelting speed, voltage, and welding current [20]. Despite the efficiency of this method, remelting is quite demanding because of the gas storage, and experienced operator [21]. Moreover, it may introduce undesirable tensile residual stresses.

The second category of the surface treatment methods comprises the residual stress improvers, which mainly aim at reducing the tensile residual stress in the heat-affected zone or even introducing compressive residual stress using an impact tool. High-Frequency Mechanical Impact (HFMI) treatment has emerged as a new and user-friendly weld improvement method for enhancing fatigue resistance. This enhancement is due to the combined effects of introducing compressive residual stress by surface cold working, increas-

ing the weld toe radius (which smoothens the weld transition), and strain hardening of the steel which reduces the susceptibility of fatigue cracks. Moreover, the treatment removes the local stress raisers at the weld toe such as undercuts which consume part of the fatigue life [21]. This treatment is given by different commercial names such as Hammer Peening (HP), Ultrasonic peening (UP), Pneumatic Impact Peening (PNP), Needle Peening (NP), Ultrasonic Impact Treatment (UIT) and High-Frequency Impact Treatment (HiFIT). The latest is preferred as it produces a finer surface finish because of the smaller spacing between the alternate impacts [22].

HFMI treatment has mainly been used on new structures, but it might have the potential to extend the fatigue life of existing structures as well. In this case, cracks may have already emerged due to fatigue loading during the service life. The performance of HFMI-treated structure depends on the treated geometry, the steel grade, the loading level, the stress ratio and last but foremost, the damage extent due to fatigue loading prior to treatment [23]. In fact, HFMI treatment has demonstrated its capability in enhancing the fatigue strength of welded details in new steel structures [24–30]. Nonetheless, less research is available on the use of this technique in fatigue life extension of welded details for existing structures [4]. This makes the performance of treated existing structures quite ambiguous and needs to be investigated thoroughly.

The fatigue strength of HFMI-treated details is known to be different from those corresponding to untreated ones (i.e. as-welded). This is the main beneficial effect of HFMI treatment from the design point of view. The international institute of welding proposed both higher fatigue strength (i.e. FAT value) and shallower slopes of the SN curve for HFMI-treated details. The introduced compressive residual stress is directly proportional to the steel grade which makes the treatment more rewarding for high-strength steel [22]. Nonetheless, the increase in fatigue strength decreases for thicker plates. Therefore, the penalty factor is assigned to the FAT value to cover this effect.

The fatigue strength of as-welded details is known to be independent of load conditions (even if this load may cause changes in residual stresses) as it is assumed that high tensile residual stresses already exist locally at the weld toe. On the other hand, the primary beneficial effect of HFMI treatment is the introduced compressive residual stress at the weld toe [31]. The stability of these stresses is an important aspect which shall be taken into consideration in the design of steel bridges treated by HFMI treatment. One aspect is the effect of load cycles with high-stress ratios which may lead to relaxation or total elimination of the beneficial compressive residual stress [32–35]. Therefore, the IIW assigns a penalty factor on the fatigue strength of HFMI-treated detail depending on the applied stress ratio [22]. However, this way is only applicable for constant amplitude loading which is not the case for bridges that are subjected to different types of vehicles or trains that generate cycles with variable amplitude. Moreover, a recent study showed that the in-service stresses cause the generation of cycles with high-stress ratios up to 0.9 which is beyond the applicability of the method suggested by the IIW to consider the stress ratio effect [5].

Another load condition that may threaten the stability of the introduced compressive residual stresses is the load peaks, or in other words, the overloads. These overloads, even if few, may also cause relaxation of the beneficial residual stress at the weld toe [36–42]. Tensile overloads are found to be less detrimental than compressive overloads. All the test results -with tensile overloads- conformed conservatively with the characteristic SN curve of HFMI treatment provided by IIW recommendation for different types of details [22]. On the other hand, some tested specimens exhibited lower fatigue strength than the characteristic fatigue strength (proposed by the IIW) when a single compressive peak load of $0.8f_y$ is applied [43]. Nonetheless, it is not yet known how to incorporate this knowledge in the design or assessment of bridges. In other words, how to make the verification of the maximum stresses (i.e. overloads) for design and assessment purposes?

One major hindrance to applying HFMI treatment on weldments in steel bridges is the

lack of design rules and recommendations such as consideration of stress ratio (or mean stress) and peak stresses (i.e overloads). This may explain why this treatment has not yet been implemented in the bridge industry on large scale. Another obstruction, particularly for existing bridges, is that the fatigue strength improvement is not well demonstrated for existing structures that have accumulated fatigue damage prior to treatment.

The fatigue damage can be expressed in different ways. For example, the Palmgren-Miner rule defines fatigue damage as the ratio between the number of applied loading cycles to the material endurance to fatigue. From a material point of view, the damage resulting from the sliding of dislocations can then accumulate to form slip bands on the surface, which –with repeated loading– are added to result in surface ridges and troughs called extrusions and intrusions [44]. In the worst case, these defects develop to form cracks. In other words, cracks are the worst form of fatigue damage. Therefore, the removal of fatigue cracks by remelting prior to HFMI treatment might influence fatigue endurance significantly. Nonetheless, this needs to be thoroughly investigated and verified.

In addition to damage and cracks, corrosion might have a detrimental effect on the fatigue performance of HFMI-treated weldments [45]. However, does this mean that the fatigue strength assigned for HFMI-treated details can be used in bridges existing in a corrosive environment? Covering all aforementioned aspects is expected to pave the way for wider implementation of HFMI treatment on new and existing welded steel bridges which thereby provides a more sustainable and economical solution for steel and composite bridges that suffer from fatigue as one of the governing states in structural design.

1.2 Objectives

HFMI treatment is a post-weld treatment method that has great potential to be used for enhancing the fatigue strength of weldments in steel bridges. The aim of the research conducted in this thesis is to provide rules and recommendations which are needed for an efficient and safe design and application of HFMI treatment on new and existing bridges. The following research objectives have been identified for this thesis:

1. Investigating the efficiency of HFMI treatment in extending the fatigue life of existing structures that have undergone some fatigue damage prior to treatment. An important research question is whether the fatigue performance of HFMI-treated details is affected by the existing fatigue damage prior to treatment. In other words, what is the extent of damage that can be tolerated prior to the application of HFMI treatment and how would this damage affect the performance of the treatment?

2. Studying the application of HFMI treatment and TIG remelting on weldments in existing structures. An important research question is about the efficiency of HFMI treatment in enhancing fatigue endurance if preceded by surface remelting using TIG remelting.

3. Studying the effect of corrosion on the efficiency of HFMI treatment. In other words, does corrosion of weldments affect the fatigue performance of HFMI-treated welds, and to what extent?

4. Providing several practical guidelines for the application of HFMI treatment on existing welded steel or composite bridges.

5. Providing a method for considering the stress ratio (i.e. mean stress) effect in HFMI-treated weldments in road and railway bridges.

6. Providing a verification format of the peak stresses (i.e overloads) for design and assessment purposes. This verification is needed to attain the beneficial compressive residual stress at the weld toe in road bridges.

1.3 Methodology

The work presented in this thesis comprises literature reviews, fatigue testing, experimental investigations, and numerical, analytical and statistical methods. The literature review have shed the light on the published fatigue test results of prefatigued welded details enhanced by HFMI treatment. Axial fatigue tests are conducted on non-load carrying transverse attachment detail in order to enhance the available knowledge on fatigue life extension using HFMI treatment. Moreover, several supportive investigations such as crack detection, local geometry scanning, residual stress investigation, hardness testing, metallurgical analysis and optical microscopy are carried out to explore the mechanisms behind life extension. Thermo-mechanical numerical analyses are conducted via the FEM-based software ABAQUS to investigate the effect of combined treatment (TIG-HFMI) on fatigue performance. Strain-based fatigue and the Palmgren Miner damage rule are used to simulate crack initiation and propagation respectively. Besides, fatigue test results are collected from different articles and analyzed to study the corrosion effect on the efficiency of HFMI-treated weldments.

Traffic data from millions of trucks and hundreds of trains are collected in Sweden and Netherlands. The data includes axle loads and configurations. The trucks and trains are run over different influence lines. The rainflow cycle counting method is used to identify the load cycles generated by the passage of these vehicles. In addition, statistical analysis and peak over threshold (POT) method are employed to determine the peak stresses carried by the steel bridge during the design life. An illustration of the methodology used in this work is presented in Figure 1.1.

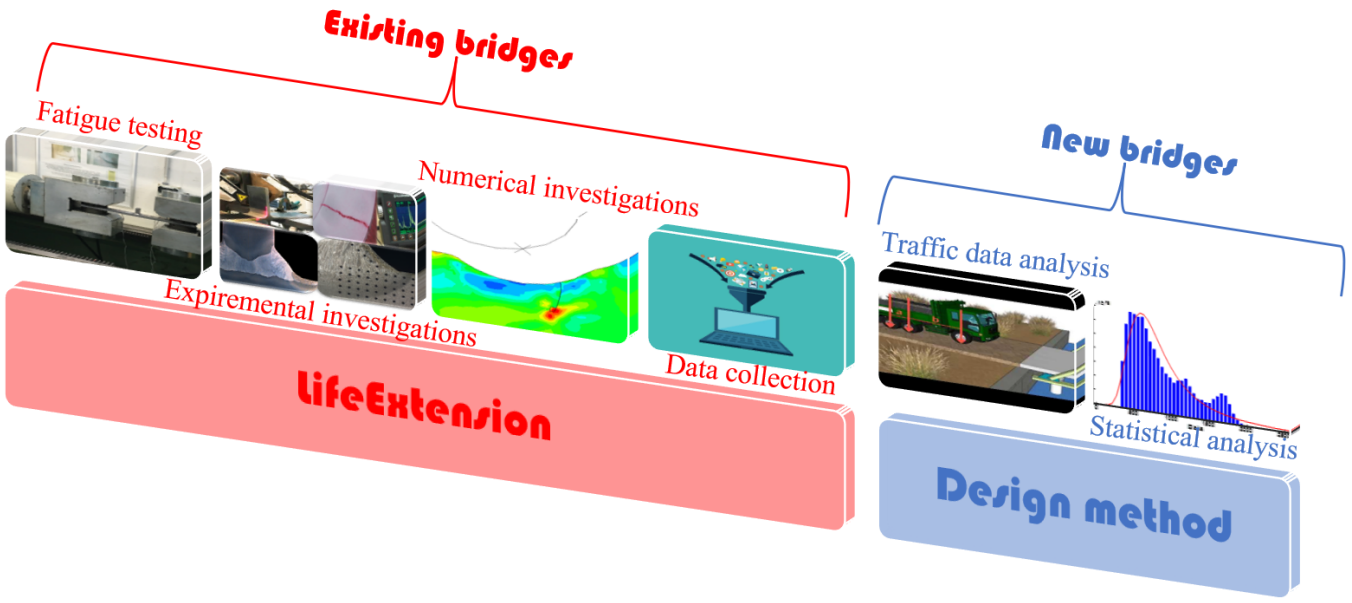

Figure 1.1: Overview of the methodology

1.4 Limitations

- The thesis focuses on fatigue improvement via HFMI treatment. TIG remelting is presented in the thesis to investigate the capabilities of the combined TIG-HFMI treatment in relation to both individual treatments. In other words, the use of TIG remelting for fatigue strength improvement is out of the scope of the thesis.
- HFMI treatment has several applications on welded structures such as aircraft, automobiles, cranes and ships. However, the results presented in this thesis regarding mean stress effects, and maximum stress limitations apply only to steel bridges.

- The investigations on the verification of maximum stresses is limited to road bridges. No similar investigations have been conducted on railway bridges.
- The design procedure proposed for the railway brides is limited to the investigated traffic pool which is relevant to Swedish traffic.

1.5 Outlines

The thesis consists of an introductory part and seven appended papers. The introductory part is divided into five sections:

Section 1: In this section, the background of the work is presented, the aim and objectives are defined, and methods, scope and limitations are outlined.

Section 2: The work conducted on fatigue life extension of existing structures is summarized. This includes fatigue testing, supportive experimental studies, numerical investigation of the combined TIG-HFMI treatment and a study on the corrosion effect of HFMI-treated details. In addition, practical guidelines are proposed at the end of this section for the applications of HFMI treatment on existing steel bridges.

Section 3: In this section, the investigations made for developing a design framework for HFMI-treated details in road and railway steel bridges are presented. This includes the consideration of mean stress (i.e. stress ratio) effects and the effect of overloads (Peak stresses). In addition, design examples are presented to illustrate how this framework can be used by engineers for design purposes.

Section 4: In this section, the main conclusions are drawn from this work and suggestions for future research are presented. A visual overview of the content of the thesis in hand is given in Figure 1.2.

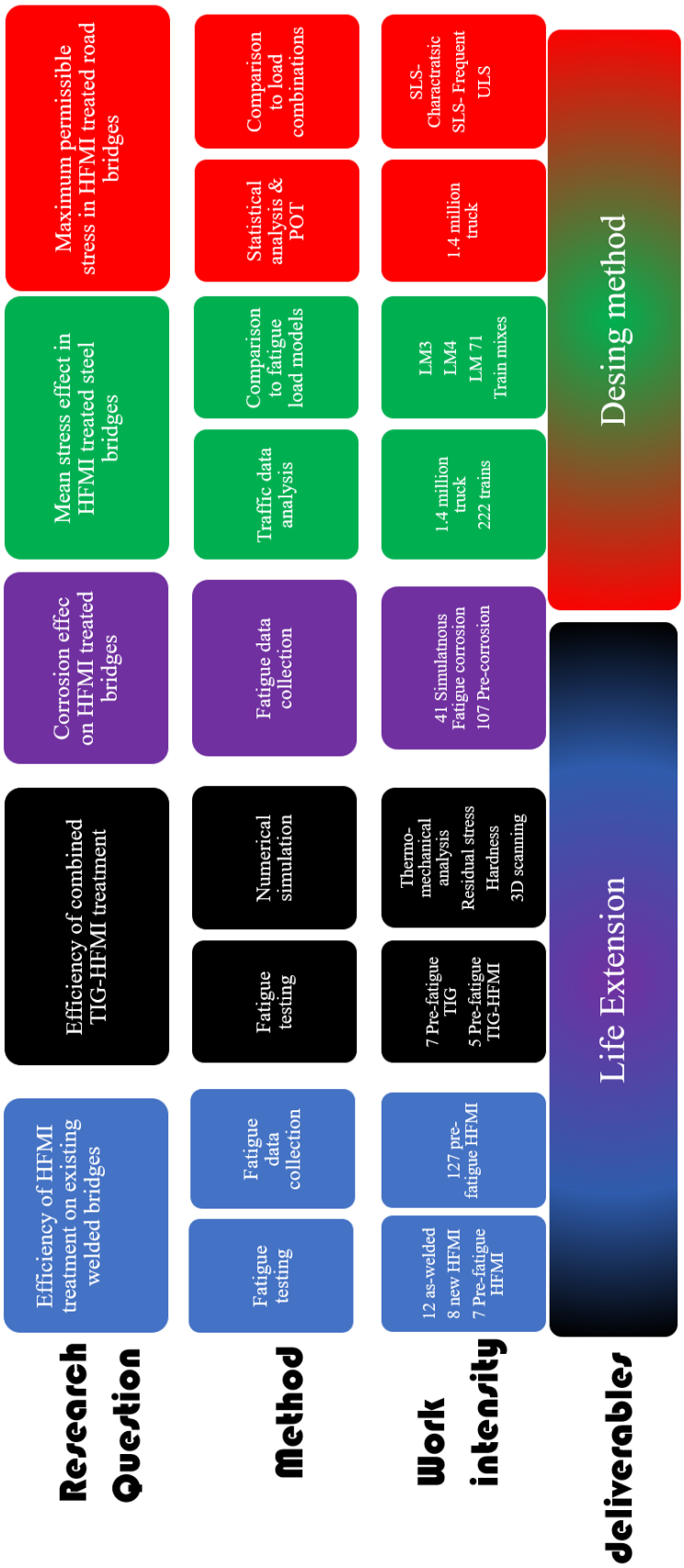

Figure 1.2: Overview of the methodology

2 Fatigue life extension of existing structures via HFMI treatment

If HFMI treatment is to be used for fatigue life extension of welded details in existing structures, the accumulated damage due to fatigue loading prior to treatment shall be taken into account. Despite that damage usually causes no, or small cracks, the effect of this damage on fatigue performance of HFMI-treated weldments is quite ambiguous [46]. Therefore, the efficiency of HFMI treatment on existing structures is investigated via fatigue testing of welded specimens. As stated earlier, the fatigue damage, in the worst case, causes the formation of fatigue cracks at the weld toe where the treatment is to be applied. Therefore, cracks have been created via fatigue loading to analogize the real fatigue cracks in structures which occurs due to loading. The cracked specimens are treated using either an HFMI indentor or a tungsten electrode to remelt the cracked region or a combination of both (TIG-HFMI).

2.1 Fatigue testing

A fatigue testing program consisting of seven series is set up. The fatigue tests are conducted on welded specimens with non-load carrying transverse attachment, see Table 2.1. The specimens in series A (as-welded) & D (HFMI-treated) are tested until failure. Besides, the specimens in series C are dedicated to microscopic investigations conducted to study the crack status after HFMI treatment which will be presented later. Besides, the specimens in series B are used to establish a correlation between the crack depth and the stiffness drop measured by attached strain gauges at the weld toe. It is found that a 20 - 25% drop in the local strain measured by any gauge is equivalent to a 0.6-1.2 mm crack. This is verified using ultrasonic scanning and destructive testing [31]. The uncertainty in the crack size is explained by the possibility of crack formation either in front of the gauge (which makes it sensed earlier) or between two adjacent gauges (which makes it sensed later).

Table 2.1: The specimens series

Series	Number	Function	Specimens	Stop criteria
A	12	Investigating the strength of the as-welded specimens	1-10, 12-13	Failure/Run-out
B	3	Crack detection and calibration	14-16	50-80% drop in strain
C	2	Investigating the crack status after HFMI treatment	17-18	50-80% drop in strain
D	8	Investigating the strength of virgin HFMI-treated specimens	21-28	Failure/Run-out
E	7	Studying the life extension by HFMI-remelting	29-35	Before treatment: 25% drop in strain After treatment: Failure/Run-out
F	7	Studying the life extension by TIG-remelting	36-42	Before treatment: 25% drop in strain After treatment: Failure/Run-out
G	5	Studying the life extension by TIG-HFMI-treatment	43-47	Before treatment: 25% drop in strain After treatment: Failure/Run-out

The effect of relatively small fatigue cracks is studied since most weldments in the existing bridge contain no or small cracks as stated earlier. Based on the correlation established between the strain drop and the crack size, the specimens in series E, F and G have been tested until a 20-25% drop in the strain (which corresponds to 0.6-1.2 mm) is reached. The specimens are then treated using the methods given in Table 2.1. Afterwards, the treated specimens are tested until failure.

Figure 2.1 shows the percentage of strain drop measured by the attached gauges in some specimens from series E, F & G. These specimens are called prefatigued specimens. It can be noticed that the number of pre-fatiguing cycles varies significantly from one specimen to another. In addition to the difference in crack formation position with respect to

the strain gauge, this can be also attributed to the individual differences between the specimens such as residual stresses, weld topography and hardness. This emphasizes that the damage is better expressed using measured crack size than the number of fatigue loading cycles.

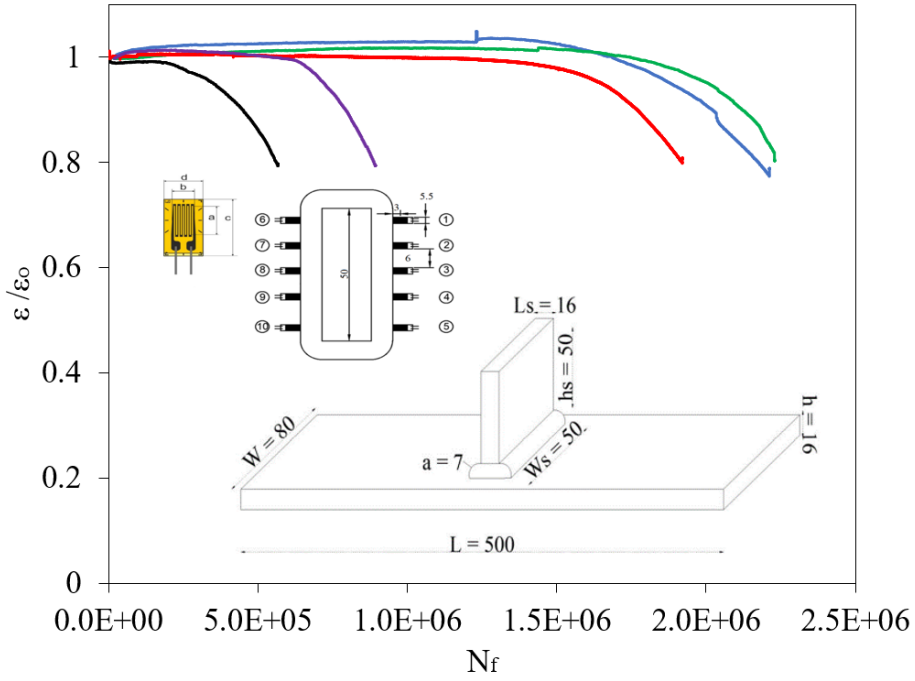

Figure 2.1: Sample of the strain measurements evolution normalized to the initial measured strain

The weld toes of the specimens in series D and E are treated using a HiFIT indentor. A single indentor tool with a 3 mm diameter is used, and the inclination angle of the indentor's axis with respect to the base plate surface is fixed to be 60-70°. This inclination in found to be appropriate even for cracked structures [47]. Besides, the toes of the specimens in series F and G are remelted by a tungsten electrode. The electrode is fit at the weld toe to achieve deeper fusion. Subsequently, a 5 mm diameter HiFIT indentor is used to treat the specimens in series G. Larger diameter should be used in order to attain the benefit of topography improvement achieved by remelting the surface.

Fatigue test results of all as-welded and treated specimens are given in Figure 2.2 & Table 2.2. The characteristic design curves of the as-welded & HFMI treated transverse stiffener (adopted from [8] & [22] respectively) are also shown in the same figure. Remarkably, the as-welded specimens show relatively high fatigue strength because of the unusual compressive residual stress existing at the weld toes. Besides, most of the treated specimens have run out after 10 million cycles when tested under a stress range of 150 MPa. All as-welded and HFMI-treated specimens fail at the weld toe, while all TIG-remelted and TIG-HFMI-treated specimens fail at the base metal from the clamping position. The effect of clamping is thoroughly studied in [48]. The obtained characteristic fatigue strengths (FAT) for as-welded, new HFMI-treated and prefatigued HFMI-treated specimens are found to be 125, 180 and 165 MPa respectively. The fatigue strength (FAT value) is calculated using the prediction interval method proposed in [49]. Besides, No FAT values are assigned for both TIG-remelted or TIG-HFMI-treated specimens as the failure has not been initiated from the weld toes.

More fatigue test results of welded structures enhanced by HFMI treatment are collected from research articles [19, 50–59]. The collection includes different detail types such as transverse attachment, longitudinal attachment, butt welds, and cover plates. In total, more than 120 data points are collected. Afterwards, A gain factor is introduced in Equa-

tion 2.6 to evaluate the efficiency of HFMI treatment in the life extension of prefatigued structures. This gain factor gives the ratio between the endurance of the prefatigued specimens, N_{EXT} to the characteristic design life of the same detail under the same stress range, N_{IIW}. The former is obtained from fatigue testing, while the latter is calculated using the SN curves for HFMI-treated details provided by the IIW [22]. N_{IIW} takes the adjustment of fatigue strength class due to plate thickness, applied stress ratio and yield strength of the material.

The gain factor is plotted against the existing crack size prior to HFMI treatment in Figure 2.3. The figure indicates that a new characteristic design life of the treated detail can be achieved if the treatment is applied when the existing crack size is not deeper than 2.25 mm. Besides, the gain factor is also plotted against another measure of damage giving the prefatigued lives normalized to the characteristic fatigue lives of the as-welded detail in Figure 2.4. The figure shows that the gain factor is always greater than 1.0 providing that the crack size is less than 2.25 mm. Therefore, it is recommended that non-destructive testing (NDT) should precede the treatment to check if the weld toe is either crack-free or contains a crack shallower than 2.25 mm.

$$G_{HFMI} = \frac{N_{Ext}}{N_{IIW}} \tag{2.1}$$

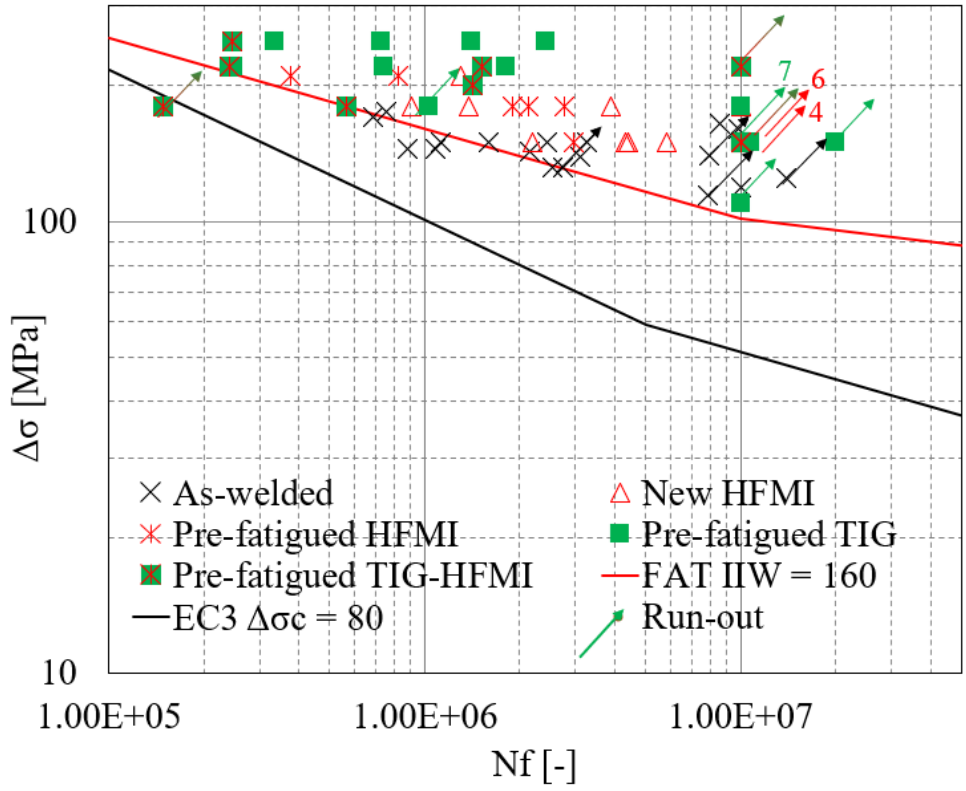

Figure 2.2: Fatigue test results of as-welded and treated specimen

Table 2.2: Fatigue tests results

Test	Specimen	$\Delta\sigma$ MPa	N Cycles	Test abort criterion	Test	Specimen	$\Delta\sigma$ MPa	N Cycles	Test abort criterion
As-welded (series A)									
A1a	1	119	1.00E7	Run-out	A4	4	145	1.08E6	Toe failure
A1b	1	143	2.15E6	Run-out	A5	5	175	7.57E5	Toe failure
A2a	2	114	7.85E6	Run-out	A6	6	170	6.85E5	Toe failure
A2b	2	125	1.04E7	Run-out	A7	7	165	8.59E6	Toe failure
A2c	2	140	8.00E6	Run-out	A8	8	160	9.87E6	Toe failure
A2d	2	132	2.75E6	Run-out	A9	9	150	1.13E6	Toe failure
A2e	2	145	8.84E5	Toe failure	A10	10	150	1.60E6	Toe failure
A3a	3	132	2.53E6	Run-out	A12	12	150	3.25E6	Toe failure
A3b	3	139	3.10E6	Toe failure	A13	13	150	2.42E6	Toe failure
Virgin HFMI-treated (Series D)									
D21a	21	180	1.00E7	Toe failure	D26	26	150	4.41E6	Toe failure
D21b	21	180	9.12E5	Run-out	D27a	27	150	1.00E7	Run-out
D22	22	150	4.32E6	Toe failure	D27b	27	180	1.38E6	Toe failure
D23	23	150	5.82E6	Toe failure	D28a	28	150	1.00E7	Run-out
D24	24	150	2.19E6	Toe failure	D28b	28	180	1.00E7	Run-out
D25a	25	150	1.00E7	Run-out	D28c	28	210	1.03E6	Toe failure
D25b	25	180	3.88E6	Toe failure					
Prefatiging stage (Series E)									
E29P	29	150	5.64E6	25% Strain drop	E33P	33	150	1.91E6	25% Strain drop
E30P	30	150	8.93E5	25% Strain drop	E34P	34	150	7.67E6	25% Strain drop
E31P	31	150	1.49E6	25% Strain drop	E35P	35	150	8.35E5	25% Strain drop
E32P	32	150	1.40E6						
Prefatigued HFMI-treated (Series E)									
E29a	29	150	1.00E7	Run-out	E32c	32	180	2.14E6	Toe failure
E29b	29	180	1.89E6	Toe failure	E33a	33	150	1.00E7	Run-out
E30a	30	150	1.00E7	Run-out	E33a	33	210	8.25E5	Toe failure
E30b	30	180	2.76E6	Toe failure	E34a	34	150	1.00E7	Run-out
E31	31	150	1.00E7	Run-out	E34b	34	150	2.95E6	Toe failure
E32a	32	150	1.00E7	Run-out	E35a	35	150	1.00E7	Run-out
E32b	32	150	1.00E7	Run-out	E35b	35	210	3.78E5	Toe failure
Prefatiging stage (Series F)									
F36P	36	150	1.92E6	25% Strain drop	F40P	40	150	5.68E5	25% Strain drop
F37P	37	150	8.15E5	25% Strain drop	F41P	41	150	6.42E5	25% Strain drop
F38P	38	150	7.66E6	25% Strain drop	F42P	42	150	2.22E6	25% Strain drop
F39P	39	150	1.27E6	25% Strain drop					
Prefatigued TIG-remelted (Series F)									
F36a	36	150	1.00E7	Run-out	F38c	38	220	7.41E5	Clamp failure
F36b	36	180	1.00E7	Run-out	F39a	39	150	1.00E7	Run-out
F36c	36	110	1.00E7	Run-out	F39b	39	220	2.49E5	Clamp failure
F36d	36	250	2.43E6	Clamp failure	F40a	40	150	1.00E7	Run-out
F37a	37	150	1.08E7	Run-out	F40b	40	250	7.29E5	Clamp failure
F37b	37	180	1.00E7	Run-out	F41a	41	150	1.00E7	Run-out
F37c	37	220	1.80E6	Clamp failure	F41b	41	250	3.34E5	Clamp failure
F38a	38	150	2.00E7	Run-out	F42a	42	150	1.00E7	Run-out
F38b	38	180	1.03E6	Run-out	F42b	42	250	1.41E6	Clamp failure
Prefatiging stage (Series G)									
G43P	43	150	5.64E5	25% Strain drop	G46P	46	150	7.18E5	25% Strain drop
G44P	44	150	8.94E5	25% Strain drop	G47P	47	150	1.35E6	25% Strain drop
G45P	45	150	1.49E6	25% Strain drop					
Prefatigued HFMI-TIG-treated (Series G)									
G48a	48	220	1.00E7	Run-out	G51a	51	150	1.00E7	Run-out
G48b	48	250	2.45E5	Clamp failure	G51b	51	200	1.42E6	Clamp failure
G49a	49	180	1.49E5	Run-out	G52a	52	180	5.65E5	Run-out
G50a	50	150	1.00E7	Clamp failure	G52b	52	220	2.41E5	Clamp failure

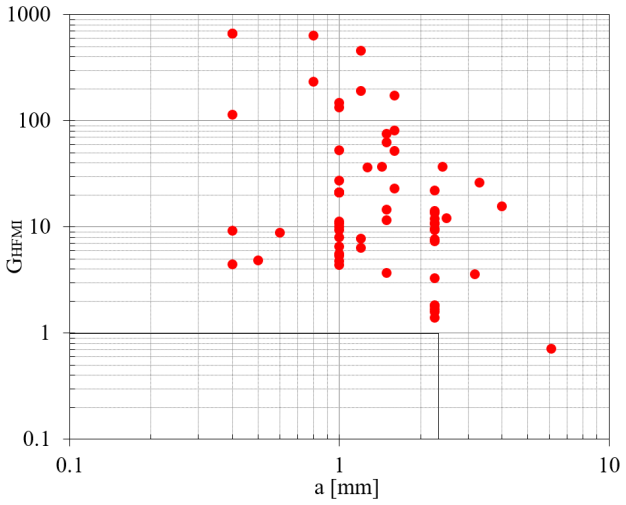

Figure 2.3: Gain factor in fatigue life versus existing crack depth

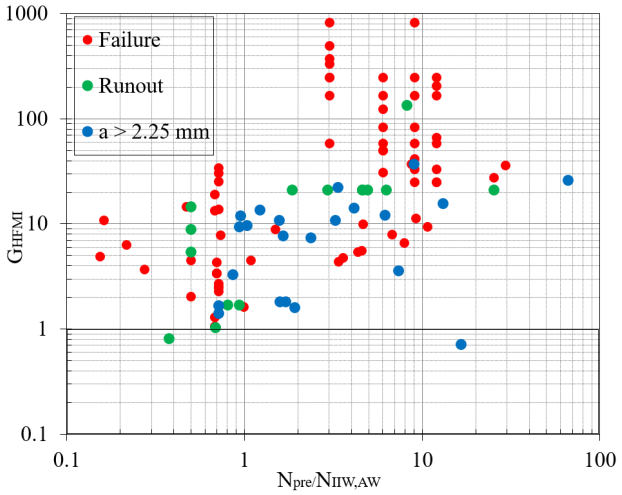

Figure 2.4: Gain factor versus pre-fatigued life before treatment normalized to the characteristic as-welded life

2.2 Supportive investigations

Figure 2.5 presents the additional supportive experimental investigations made in this section. Exploring the advantages and disadvantages of combining TIG remelting with HFMI treatment requires a deep understanding of the mechanisms behind fatigue strength improvement. These mechanisms usually counteract the detrimental effects induced by welding or loading.

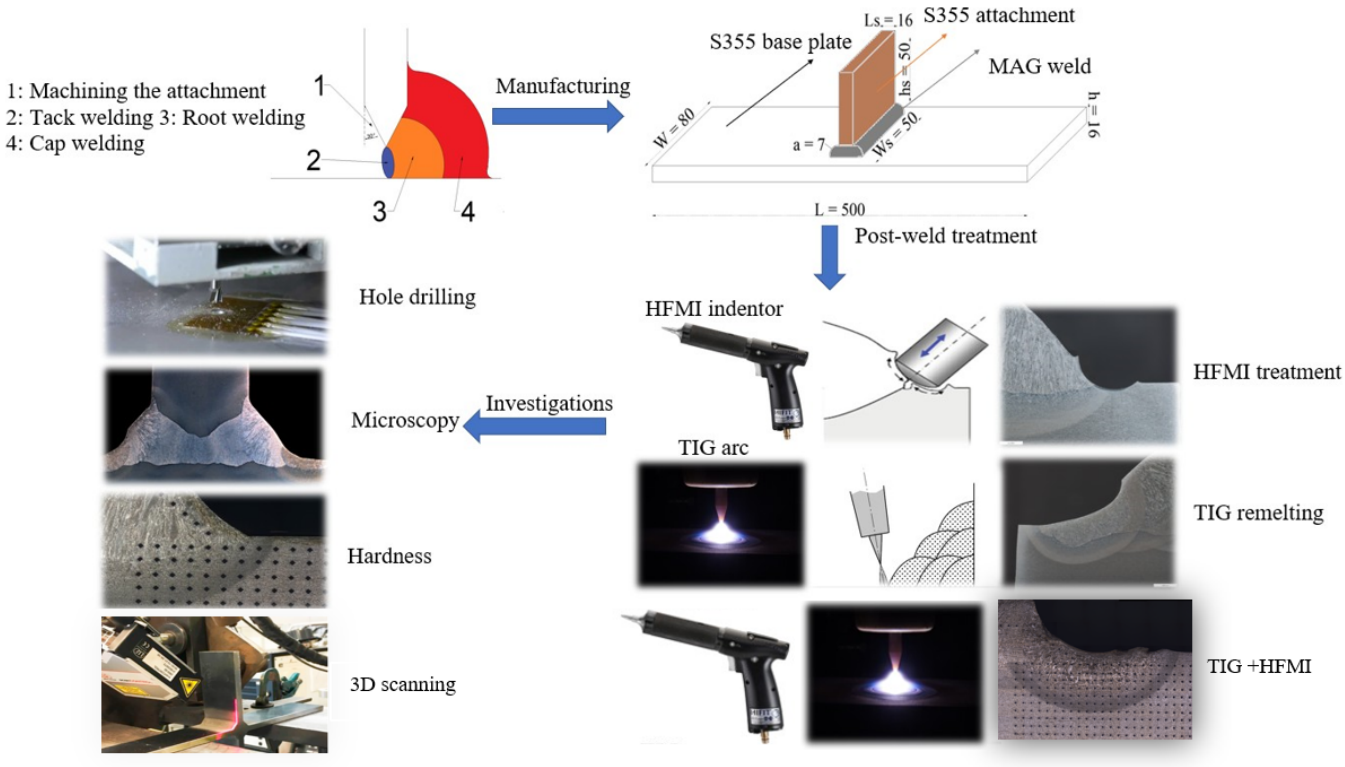

Figure 2.5: Supportive experimental investigations on treated specimens

2.2.1 Local topography investigations

Because of the importance of local geometry in evaluating the efficiency of the studied treatment methods, several specimens are scanned by a 3D laser scanner before and after treatments (i.e. HFMI-treatment, TIG-remelting, combined TIG-HFMI-treatment). Three geometrical parameters are studied: toe radius, undercut depth and HFMI groove depth, see Figure 2.6, 2.7 & Table 2.3. A significant reduction in the coefficient of variation of the radius is observed after all treatment methods which demonstrates the treatment uniformity.

Table 2.3: The geometrical parameters of the tested specimens before and after treatments

Status	AW		HFMI		TIG		TIG-HFMI	
Geometrical parameter	Toe radius	Undercut heigh	Toe radius	Groove depth	Toe radius	Undercut heigh	Toe radius	Groove depth
Mean [mm]	0.67	0.004	1.2	0.26	5.09	0.150	5.39	0.14
Standard deviation [mm]	0.31	0.03	0.29	0.13	0.73	0.10	2.44	0.06
Variation coefficient [-]	0.46	8.74	0.24	0.51	0.14	0.67	0.45	0.41
Population size [-]	20660	20660	1331	1653	150	1581	334	351

The average groove depth of the HFMI-treated specimen is 0.26 mm which is within the

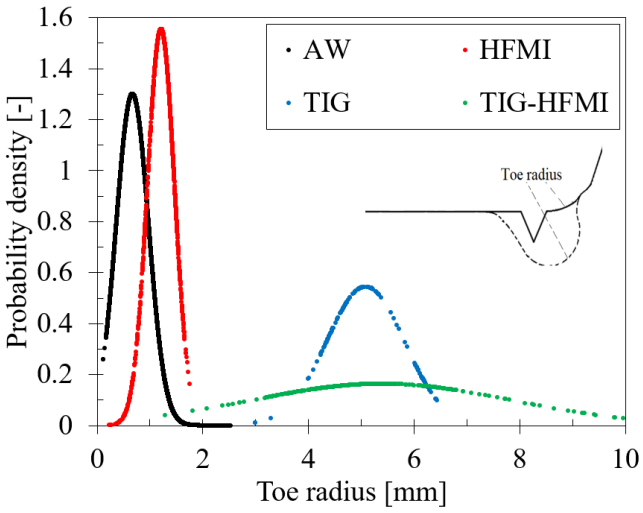

Figure 2.6: Normal distribution of weld toe radius before and after different studied treatment methods

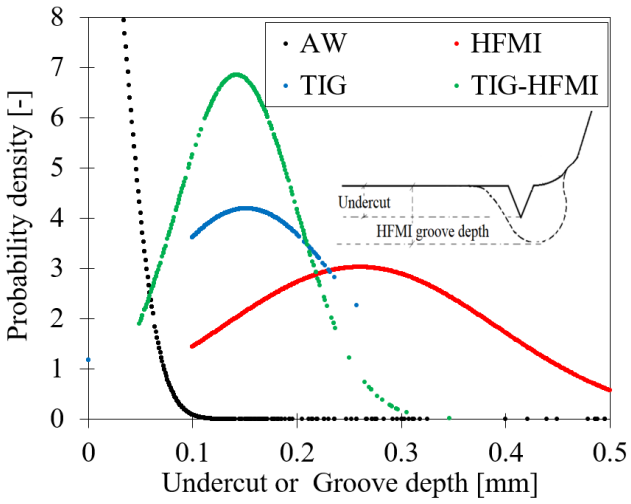

Figure 2.7: Normal distribution of undercut height (for AW & TIG) and groove depth (for HFMI & TIG-HFMI)

approved interval set by the IIW recommendations [22]. TIG-remelting causes a more significant increase in the toe radius with a factor of 7. However, fitting the electrode at the weld toe to secure deeper fusion at the crack plane causes the formation of larger undercut at the new weld toe position. Moreover, a larger HFMI-indentor is used for combined TIG-HFMI-treatment (i.e. 5 mm diameter instead of 3 mm) in order to attain the improvement in local geometry achieved by the preceding treatment (i.e. TIG-remelting).

The effect of the improved radius on the stress concentration factor is studied numerically using the commercial software ABAQUS. The effective notch stress is calculated using a reference toe radius of 1 mm in as-welded condition and the average measured toe radius + 1 mm after treatment [60, 61]. Different fatigue strength values would be assigned for each treatment method if the concentration factors are to be used for fatigue strength assessment using the effective notch method [62]. However, this is out of the scope of this thesis. The obtained stress concentration factor distributions in the top 1 mm from the surface are shown in Figure 2.8.

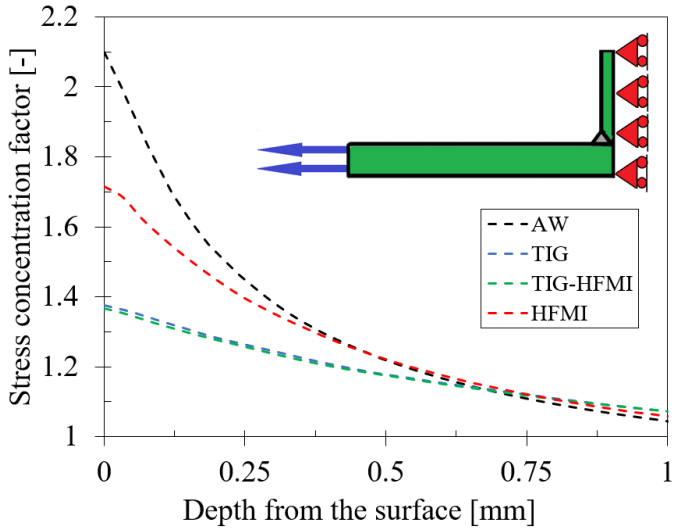

Figure 2.8: The elastic stress concentration factors

Table 2.4: Residual stress measurement results

Status		Maximum σ_{RS} [MPa]	Depth of maximum σ_{RS} [mm]
Average	AW	-185	0.10
	HFMI	-375	0.24
	TIG	-257	0.10
	TIG-HFMI	-613	0.18
Maximum	AW	-265	0.10
	HFMI	-430	0.28
	TIG	-290	0.07
	TIG-HFMI	-738	0.18
Minimum	AW	-104	0.10
	HFMI	-330	0.18
	TIG	-209	0.07
	TIG-HFMI	-413	0.13

2.2.2 Residual stress measurements

The residual stress of different specimens is investigated using the hole-drilling technique. In each specimen, the attachment is first cut parallel to the loading direction in order to allow for better accessibility of the hole drilling tester. Two reference points are measured before and after cutting to verify that cutting has no effect on the status of residual stress. The two measurements are fairly similar, which implies little or no effect of cutting. The holes are drilled at the weld toes of both the as-welded and TIG-treated specimens and at the edge of the HFMI groove of both HFMI-treated and TIG-HFMI-treated specimens.

The measured residual stresses are plotted in Figure 2.9. Remarkably, compressive residual stress is found at the weld toes even in the as-welded condition. This explains the high fatigue strength that was observed for the as-welded specimens. Nonetheless, the maximum obtained compression becomes significantly larger after HFMI treatment. This indicates that HFMI treatment is beneficial regardless of the status of residual stresses in as-welded conditions. Moreover, the maximum obtained compression after HFMI-treatment & TIG-HFMI-treatment is found at a depth of 0.15-0.30 mm which is the depth of the HFMI groove, see Table 2.4, which summarizes the findings.

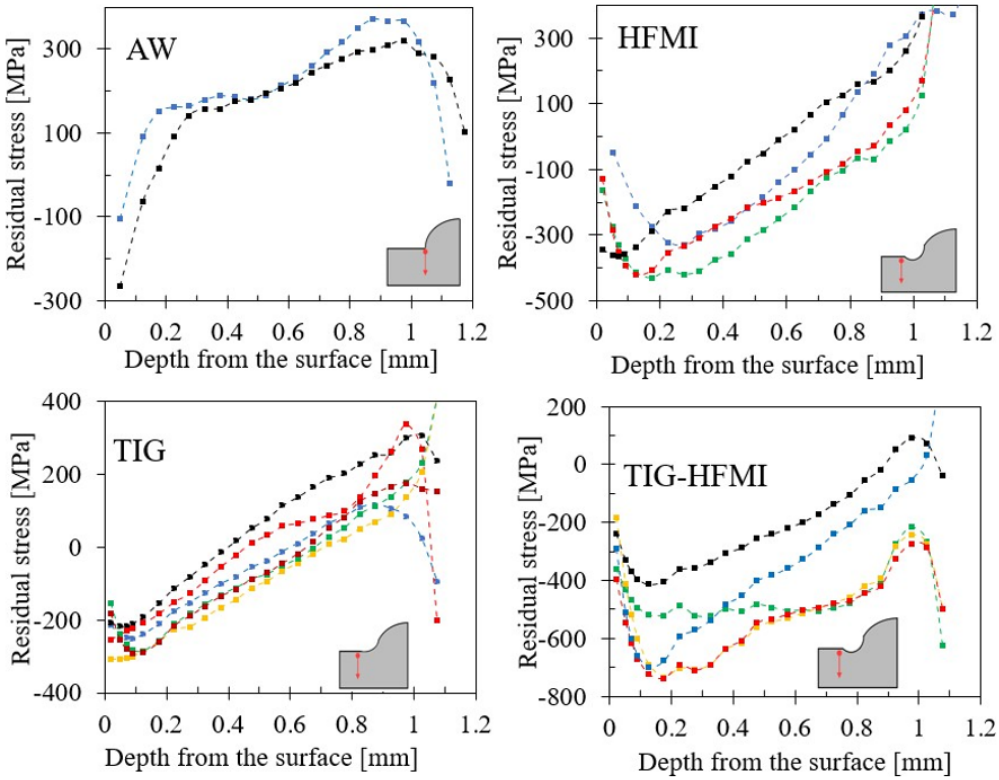

Figure 2.9: Residual stress measurements for specimens in different status

2.2.3 Local hardness measurements

Vickers tester is used to evaluate the hardness contour in the vicinity of the weld toe. A test load of 3 Kg is used, and rectangular grids are considered with a spacing of 0.5 mm both horizontally and vertically. The hardness distribution at the weld toe vicinity is shown in Figure 2.10, and the values are extracted below the weld toes and presented in Figure 2.11. The hardness increases significantly at the weld toe because of HFMI indentation. Moreover, TIG-remelting causes a further hardness increase in the heat-affected zone when succeeded by HFMI treatment with a larger indentor. TIG-remelting alone does not cause the same increase in the weld toe's hardness, but it affects a deeper area.

2.2.4 Numerical investigation on fatigue strength improvement

In order to further understand how the above-mentioned local changes (residual stress, microhardness, and topography) affects the fatigue endurance of welded details, several finite element simulations have been conducted for the different treatment process. The focus is on the combined TIG-HFMI treatment, but both individual treatments are also simulated for the sake of comparison. 2D models are adopted for the simulation with plane strain conditions. The commercial software Abaqus is used to conduct the numerical analysis needed for the stress evaluation after treatment (TIG remelting, HFMI treatment or both), and after applying the fatigue loading.

Thermo-mechanical simulations are conducted to evaluate the residual stress introduced by TIG-remelting. The measured heat input from TIG remelting is prescribed, and the ambient temperature is assumed to be at room temperature. Abaqus Welding Interface (AWI) is used to connect the temperature distribution (obtained from the thermal analysis) to the thermal contractions and expansions (in the mechanical analysis). The analyses are terminated when the temperature reaches the ambient temperature, which indicates the end of the cooling stage. The modelled weld toe radii are taken as the mean values

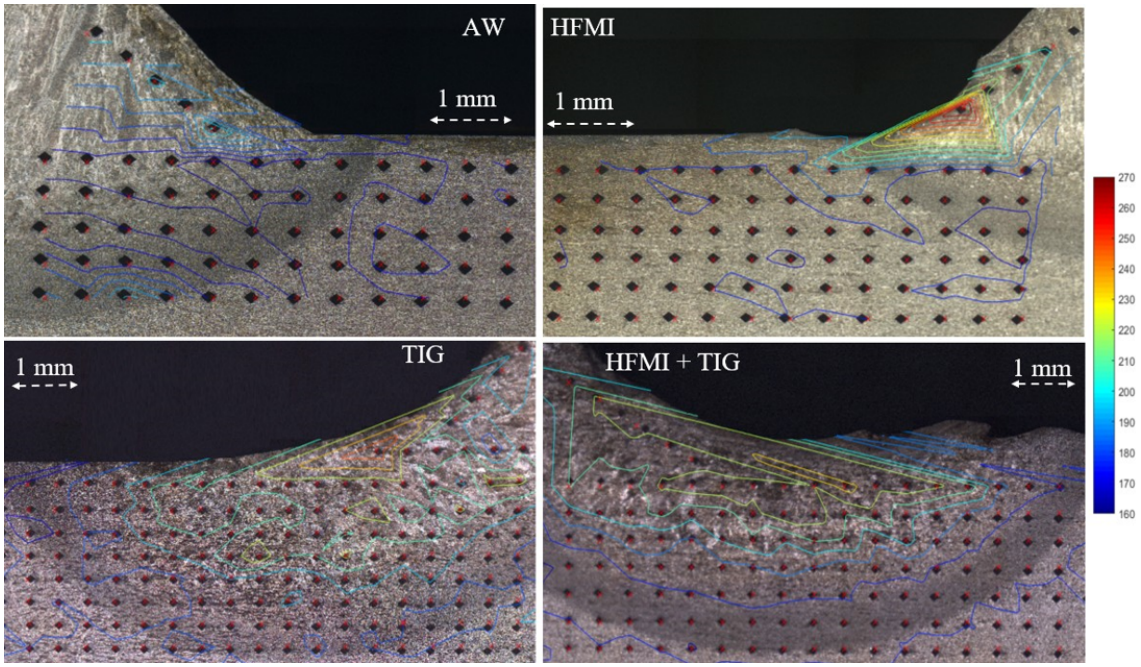

Figure 2.10: Vickers hardness distribution before and after treatment

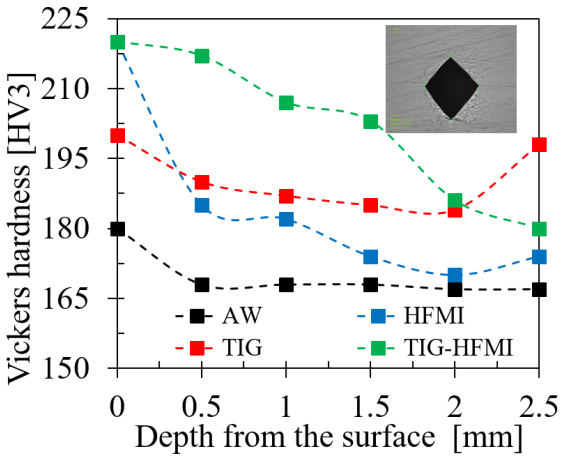

Figure 2.11: Vicker's hardness distribution below the weld toe

presented in Table 2.3. 2D models are adopted to simulate the TIG torch under plane strain conditions. Half of the geometry is modelled benefiting from the symmetry line. Four-noded linear quadrilateral elements are used to create the mesh. An element size of 3 mm is selected, and based on the convergence study, the mesh is refined to 0.1 mm for the region in the weld toes vicinity.

For HFMI treatment, two indentors sizes are used: one for the combined treatment (ϕ = 5 mm), and another smaller one for HFMI treatment alone (ϕ = 3mm). Besides, a friction coefficient is assumed between the deformable specimen and the rigid undeformable indentor. The depth of penetration is prescribed to be 0.26 mm and 0.14 mm for the 5 mm and 3 mm indentors respectively. These values are also obtained from the measurement given in Table 2.3. Furthermore, an additional boundary condition is assumed to simulate the fastening of the specimen during treatment. This boundary condition is eliminated after treatment. The models are described in Figure 2.12.

The treated specimens have then been subjected to pulsating membrane stress with a stress range of 180 MPa, and a stress ratio of 0.29, analogously to the fatigue testing given in

Section 2.1. Then, the fully reversed stress range $\Delta\sigma_{Loc}$ is calculated for each element in the mesh as given in Equation 2.2. In this equation, $\Delta\sigma_{Loc}$ and $\sigma_{m,Loc}$ are the local stress range and mean stress obtained from the FEM model, while $\sigma_{u,L}$ gives the local ultimate strength obtained from the hardness measurement given in Figure 2.10. σ_{RS} gives the residual stress. $\Delta\sigma_{Loc}$ expression is adopted from the mean stress correction suggested by Goodman [63].

$$\Delta\sigma_{ar} = \frac{\Delta\sigma_{Loc}}{1 - \frac{\sigma_{m,Loc} + \sigma_{RS}}{\sigma_{u,L}}} \tag{2.2}$$

$$\frac{\sigma_{RS}}{\sigma_{RS,1Cycle}} = N_i^k \tag{2.3}$$

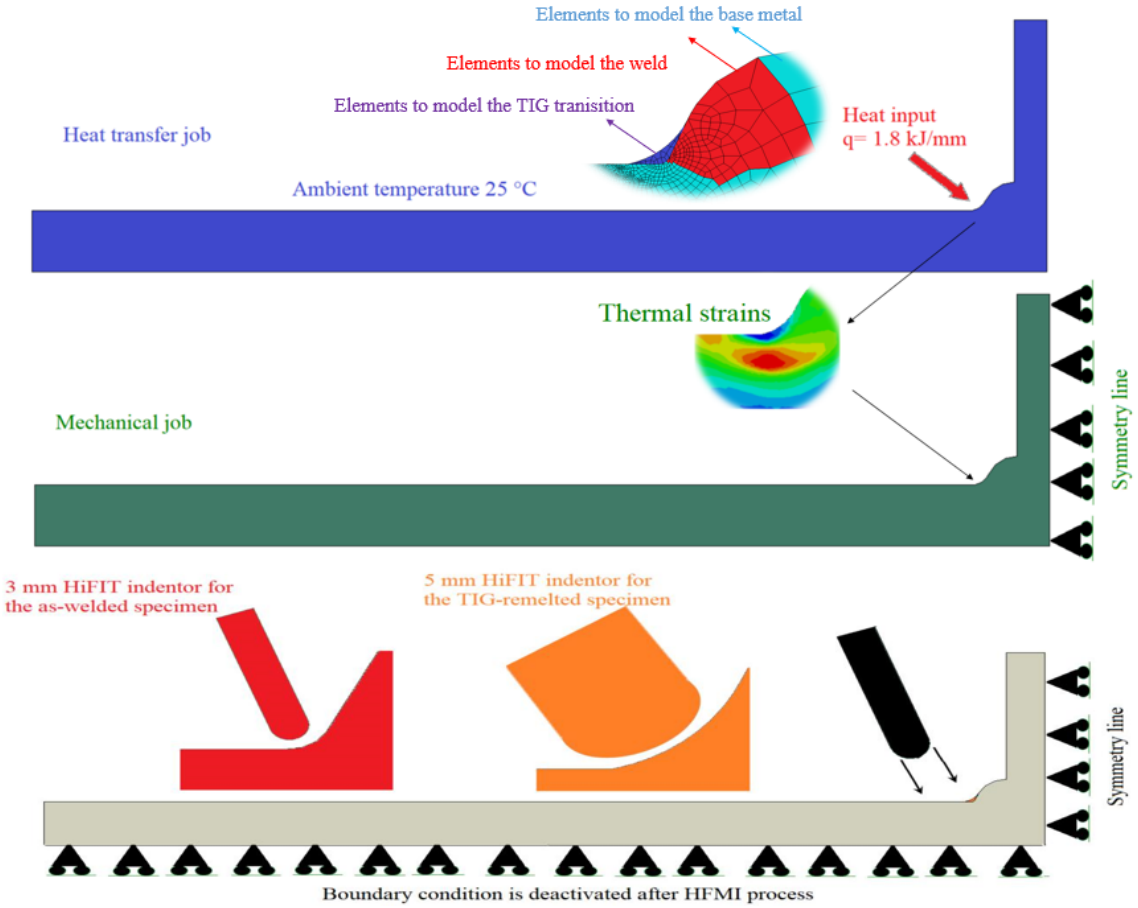

Figure 2.12: Description of the finite element model used to obtain the residual stresses after TIG-remelting and HFMI treatment

It should be noticed that the residual stresses change continuously during fatigue loading. In the conducted analyses, three stages of residual stress change are taken into account. The first is considered explicitly by applying one load cycle after treatment which causes partial relaxation. The obtained residual stress then is called $\Delta\sigma_{RS1cycle}$. Then, continuous relaxation occurs during fatigue loading until crack initiation as given in Equation 2.3, where *k* is an empirically evaluated exponent. Subsequently, residual stress keeps changing due to crack propagation. The strain and the endurance of each finite element are calculated via Equations 2.4 and 2.5 respectively.

The damage in the finite elements is then calculated as the ratio between the endurance of each finite element to the endurance of the weakest element (i.e. element with the least endurance). The damaged elements are then removed, and crack propagation has already

occurred. It should be noticed that the relaxed residual stress used to evaluate the strain is based on assuming the crack initiation life which implies that the assumed life should be compared to the obtained life, and the relaxed residual stress is changed until the difference becomes insignificant. In other words, evaluating the crack initiation life is an iterative process. The described analysis is summarized in the flowchart given in Figure 2.13.

$$\Delta\epsilon = \begin{cases} \frac{\Delta\sigma_{ar}}{E} + K.(\frac{\Delta\sigma_{ar}}{E})^n, & \text{if } \Delta\sigma_{ar} \geq \sigma_{y,L} \\ \frac{\Delta\sigma_{ar}}{E}, & \text{otherwise} \end{cases} \tag{2.4}$$

$$\frac{\Delta\epsilon}{2} = \frac{\sigma_f^{'}}{E}.(2.N_f)^b + \epsilon_f^{'}.(2.N_f)^c \tag{2.5}$$

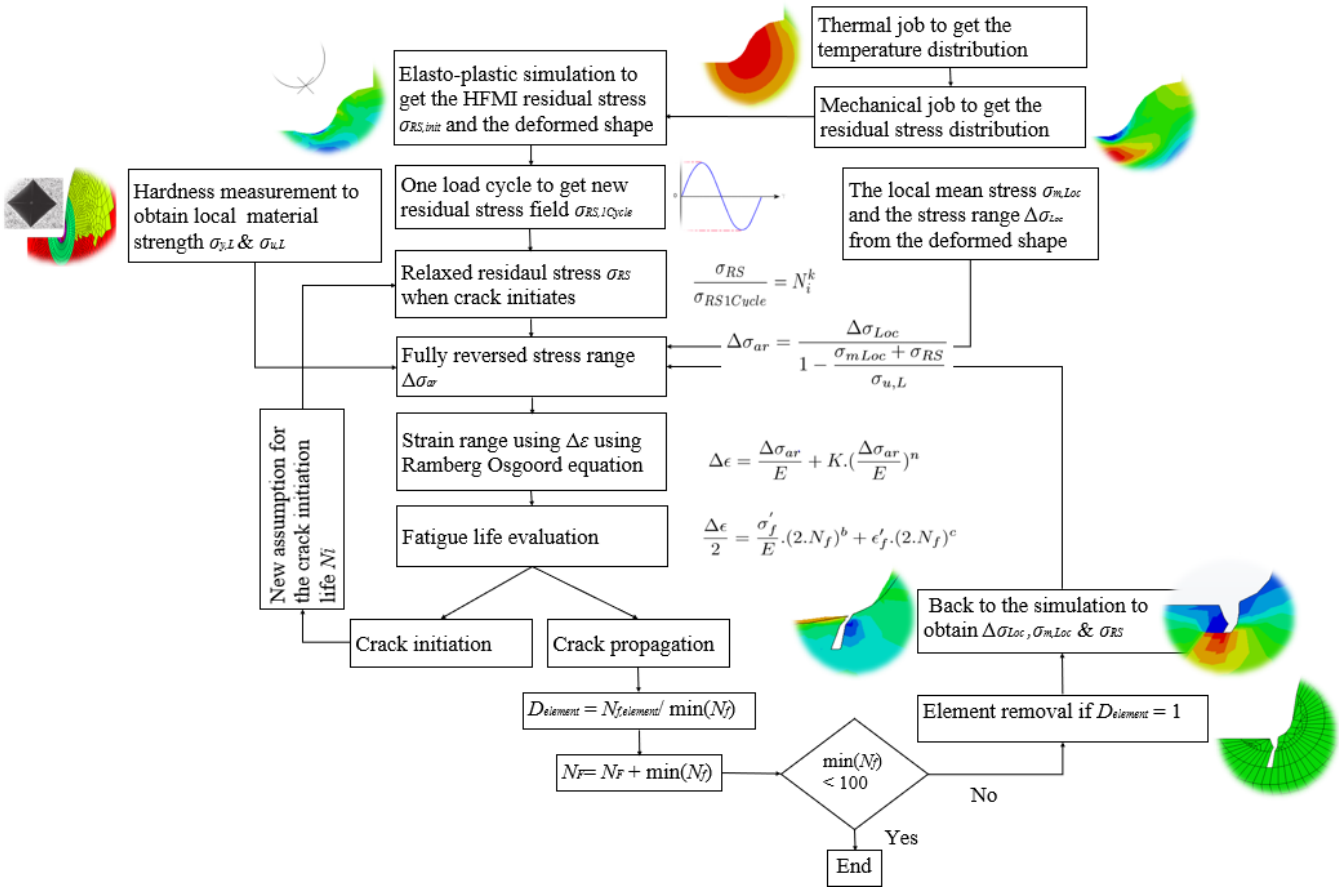

Figure 2.13: Flowchart for fatigue life analysis

The residual stresses induced by welding are not considered in the analysis. This simplification is motivated by the post-weld treatment, which changes residual stress significantly. Moreover, the inclusion of residual stress does not consider the phase transformation in the material due to mechanical or heat treatment which affects the mechanical properties of the material. Therefore, the hardness measurements are considered explicitly in the analysis to take the change in material strength caused by treatment into account.

The number of cycles to failure is plotted versus the crack size in Figure 2.14. Again, the combined treatment causes a remarkable fatigue life extension, 40% longer than the life of the HFMI-treated specimens. This could not be verified experimentally as all the combined treated details have failed from the base metal as stated in Section 2.1. Therefore, fatigue test results of transverse and longitudinal attachments treated by combined

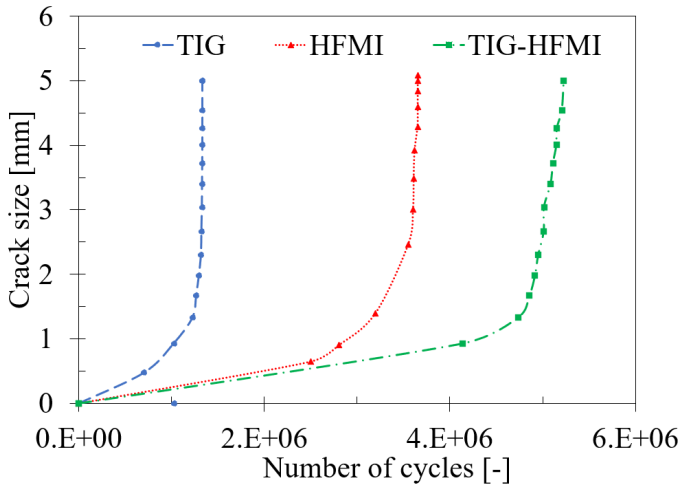

Figure 2.14: Crack propagation curves

TIG-HFMI treatment are collected from relevant research articles [26, 27, 64]. The data pool corresponds to steel with different yield strengths ranging from 355 to 900 MPa, see Figure 2.15. The results clearly show that a fatigue strength of around 180 MPa is obtained for both detail types (transverse and longitudinal attachments). This is the absolute maximum possible fatigue strength assigned to any detail treated by HFMI treatment according to the IIW which is even higher than the fatigue strength assigned for the base metal.

The above-mentioned analyses verify the potential of combined TIG-HFMI treatment in

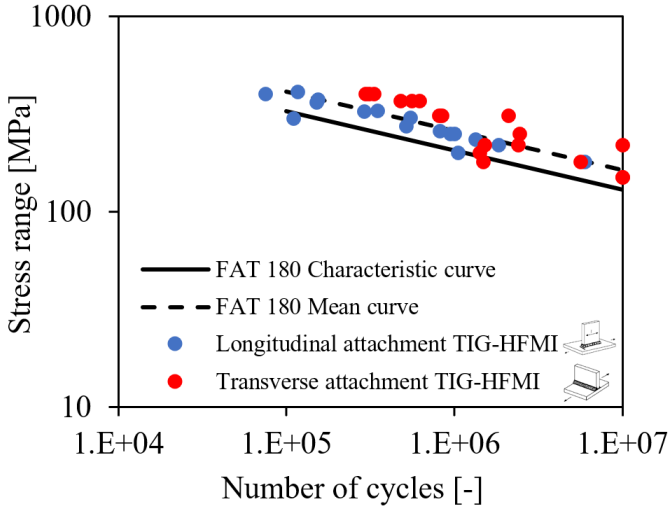

Figure 2.15: Fatigue test results of transverse and longitudinal attachments treated by combined TIG-HFMI treatment

enhancing the fatigue strength of new structures. Nonetheless, TIG-HFMI combination can be more useful if applied to existing structures which have exhibited fatigue cracks. In this case, TIG remelting causes crack removal (providing that the crack size is smaller than the fusion depth) and HFMI treatment removes the generated undercut and induces further compressive residual stress as shown in Figure 2.9.

The removal of fatigue cracks by TIG-remelting depends on both the crack depth and the fusion depth as stated earlier. If the crack is deeper, part of the crack will remain after remelting. However, this effect might be different if TIG remelting is followed by HFMI treatment. Therefore, the analysis given in Figure 2.13 is adjusted to include a 3 mm

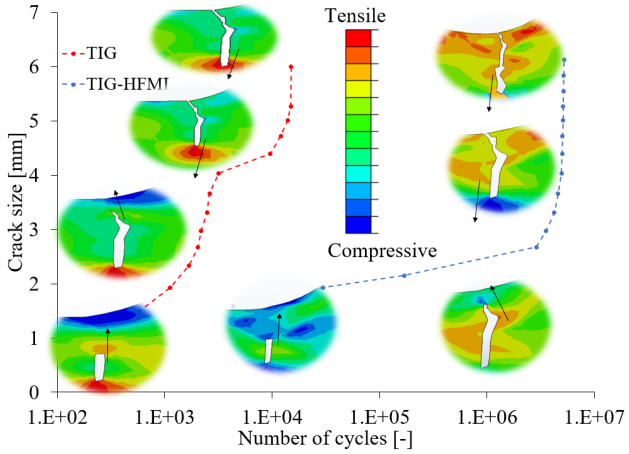

Figure 2.16: Comparison between the fatigue life after TIG-remelting and TIG-HFMI treatment

fatigue crack. A fusion depth of 1.8 mm is assumed based on metallurgical analysis conducted in [47] on the same type of details. Therefore, several finite elements are removed underneath to simulate the remaining crack which is 1.25 mm deep. The analyses are conducted on both TIG-remelting and combined treatment.

For both treatment methods, cracks have not re-initiated from the weld toe, but they prop-

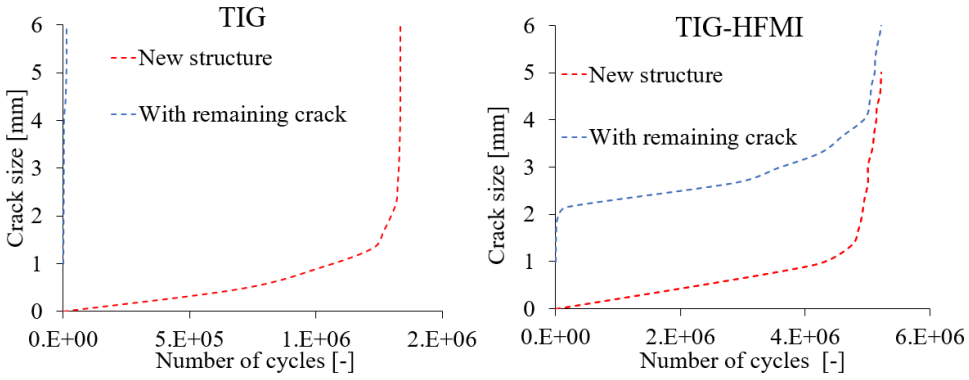

Figure 2.17: Comparison between fatigue life of new and cracked details treated by TIG-remelting and combined treatment

agate upwards from the remaining crack until they reach the surface, and then quickly propagate from the other tip downwards. Figure 2.16 clearly shows that the remaining life is significantly extended by HFMI treatment, even if the crack initiation position is altered. The slope change indicates the switch in crack propagation from upwards (i.e. toward the surface) to downwards. In fact, the fatigue lives of details treated by combined TIG-HFMI are very similar to those obtained for uncracked details in contrast to TIG remelting as shown in Figure 2.17. This can be explained by the induced compression at the crack tip after HFMI treatment. However, this effect decreases as the embedded crack becomes deeper than 2.25, see Figure 2.18. This corresponds to a total crack depth of 4 mm before treatment. On the other hand, HFMI treatment alone induces compressive plasticity only for cracks no deeper than 1.5 mm [31]. Besides, a literature study on residual stress measurements has shown that it is unlikely to induce compressive residual stresses deeper than 2 mm from the surface of the treated weldments.

Applying HFMI treatment after TIG remelting should not be practically difficult to implement as HFMI is a cheap, fast, lightweight and easy-to-operate treatment compared to TIG remelting. Therefore, it should be decided when TIG remelting is not needed. For existing structures, non-destructive testing (NDT) is required to check fatigue cracks at

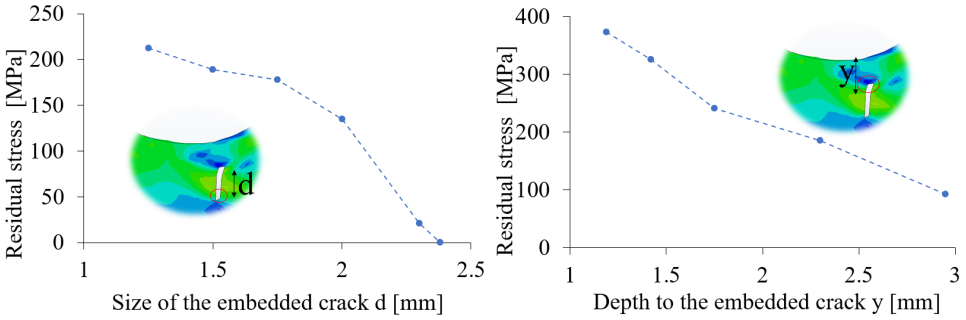

Figure 2.18: Embedded crack size effect on the compressive residual stress

the surface. One of the simplest NDT methods is to apply a crack revealer such as a dye penetrant or magnetic particles [4]. However, these kinds of methods do not have the capability of measuring the crack depth. If the crack revealer shows no crack at the surface, then there is no crack to be fused, and TIG remelting is not even needed.

On the other hand, if the crack revealer shows a crack on the surface, a more accurate NDT method (such as ultrasonic testing) is required to determine the crack depth. Besides, similar welded detail should be manufactured, and treated by TIG remelting with specific parameters (i.e. voltage, current, speed and heat input) in order to secure that the fusion depth is larger than the crack size. This verification is to be made via metal inspection. Due to the inherent inaccuracies in crack detection, the estimated crack depth can be smaller than the real one [20]. Nonetheless, subsequent HFMI treatment can put the possibly remaining crack under compression which increases the fatigue endurance as shown in Figure 2.17. In fact, the combined treatment can be used even if a 2 mm crack remains after treatment. However, the accuracy of the measurement should be well established in this case. It should be noticed that if the treatment is to be applied to a new structure, HFMI treatment is sufficient, and the complexity of TIG remelting could be avoided.

When the combined treatment is to be applied to an existing structure containing cracks, the tungsten arc should be placed right at the weld toe even if this practice leads to new undercut formation. Fitting the electrode at the weld toe secures that the position where the maximum fusion is reached corresponds to the crack plane. In other words, crack removal should be prioritized over geometry optimization. On the other hand, if the combined treatment is to be applied on a crack-free structure (which is not advised as HFMI treatment is sufficient), the electrode is to be placed at 1-2 mm from the weld toe to provide a smoother transition and avoid the risk of new undercut formation [17]. Besides, in combined treatment, a larger HFMI indenter size should be used to attain the improvement in the local topography achieved by remelting. Finally, the indenter should be inclined more to the base metal to ensure the flow of material toward the crack [31].

2.2.5 Microscopic investigations

Since the effects of HFMI treatment are local, a microscopic investigation is needed to observe the micro-structural changes and the crack status after treatment. Accordingly, some cracked specimens are first prepared by cutting them parallel to the weld line and slicing the remaining perpendicularly. The obtained surfaces of the slices are processed by polishing and Nital-etching.

The produced slices used for the microscopic investigations contain cracks of different sizes. The crack width (i.e. the distance between crack surfaces) decreases significantly after HFMI treatment (the average value decreased from 0.05 mm to 0.01 mm). In some cases, the cracks are so faint to an extent that they could not be distinguished from the grain boundaries indicating the narrowness of the crack. However, only the top part of the crack is affected by the mechanical impact if the crack is deep. Besides, the orientation of

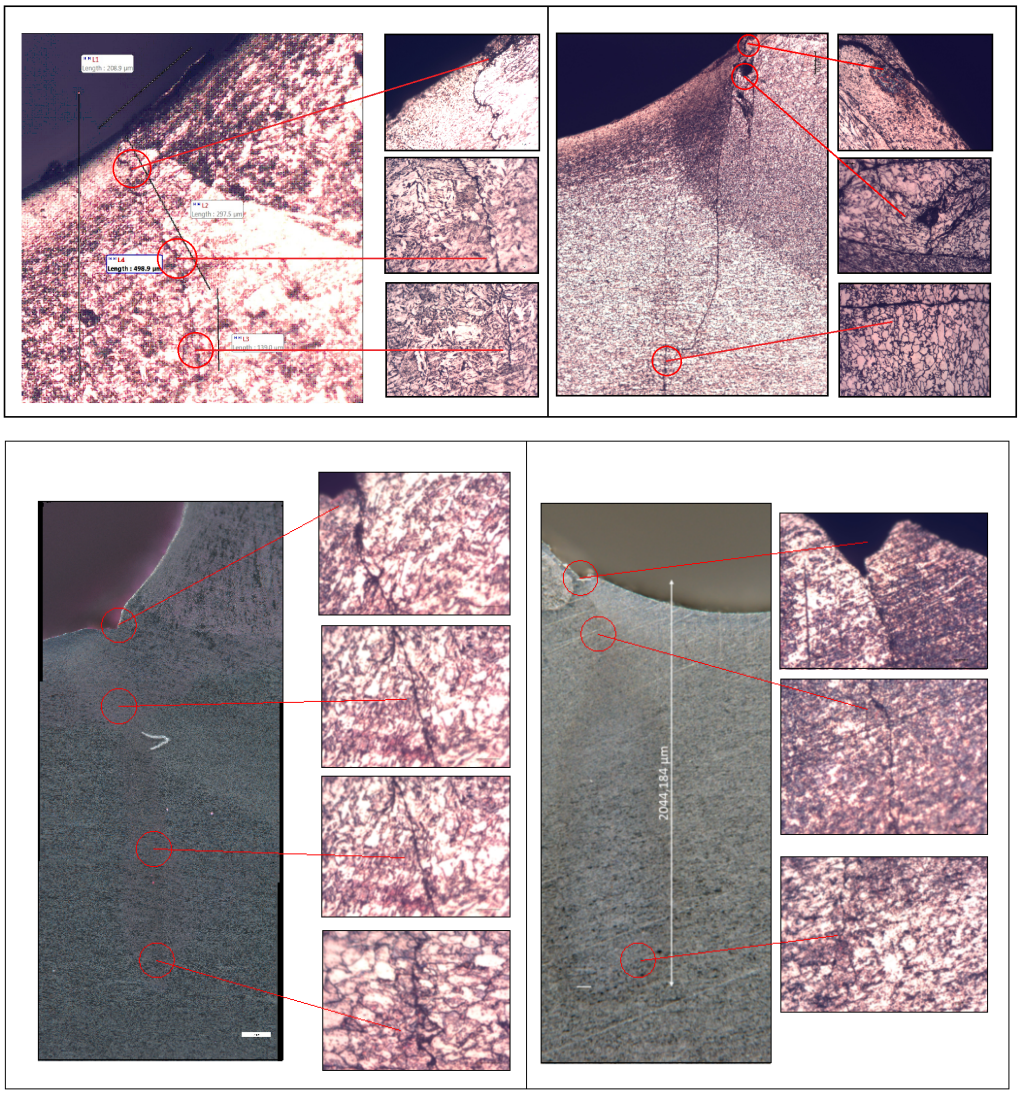

Figure 2.19: Observations of the cracks shapes after HFMI-treatment for different specimens
Top: The change in crack orientation due to HFMI-treatment.
Bottom: The top layer was not closed due to misalignment of the indentor.

fatigue cracks is observed to be changed due to HFMI indentation. Moreover, the indentor might miss the top few micrometres of the crack. These observations are shown in Figure 2.19 and more details can be found in [31].

2.2.6 Corrosion effect on HFMI treatment

Corrosion is a degradation phenomenon that poses a threat to the durability of metallic structures. The rate of corrosion in steel structures is known to be dependent on the corrosive environment, duration of exposure and steel grade [65]. Besides, corrosion causes a remarkable reduction in fatigue resistance of welded details due to its localization at the weld line [66]. Therefore, paint is usually applied to protect the steel, and inspection intervals are assigned to check the adequacy of the protection layer because it may fail due to inappropriate application. However, some parts of the structure may not be accessible to perform the inspection. Therefore, the effect of corrosion on fatigue strength improvement due to HFMI treatment needs to be investigated, not least that corrosion causes the removal of the surface layer which is the most improved in terms of compressive residual stress and hardness [67].

More than 150 fatigue test results have been collected from several research articles [45, 67–74]. The tests are conducted at a room temperature. In order to resemble the corrosive medium, the HFMI treated specimens are either fatigue-tested in a corrosive medium (i.e. simultaneous fatigue-corrosion) which resembles new structures or soaked in the corrosive medium for a specific time before fatigue testing (i.e. pre-corrosion test) which better resembles existing structures that have already undergone certain corrosion damage.

The effect of corrosion on the efficiency of HFMI treatment for pre-corroded details is evaluated using a gain factor. This gain factor gives the ratio between the fatigue life of the treated corroded detail (obtained experimentally) to those of the treated uncorroded detail (also obtained experimentally), see Equation 2.20. This gain factor is plotted against the corrosion level represented by the concentration of corrosive medium multiplied by the time exposures expressed in hours, see Figure 2.20. An inverse correlation is found between the corrosion level and the gain factor which might be explained by the progressive layer removal from the surface of the treated details where the indeuced compressive residual stress dominates.

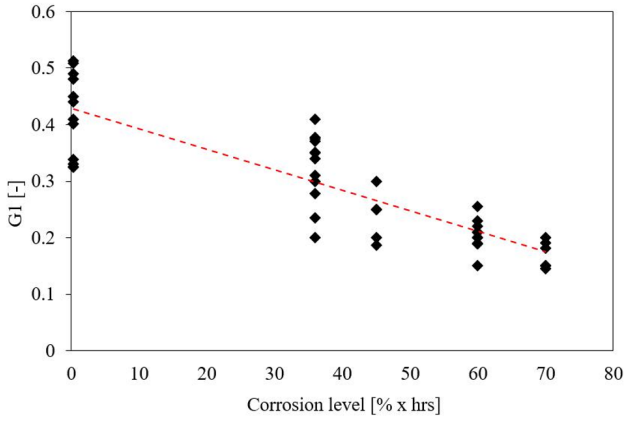

Figure 2.20: Corrosion level effect on the efficiency of HFMI treatment (Pre-corrosion tests)

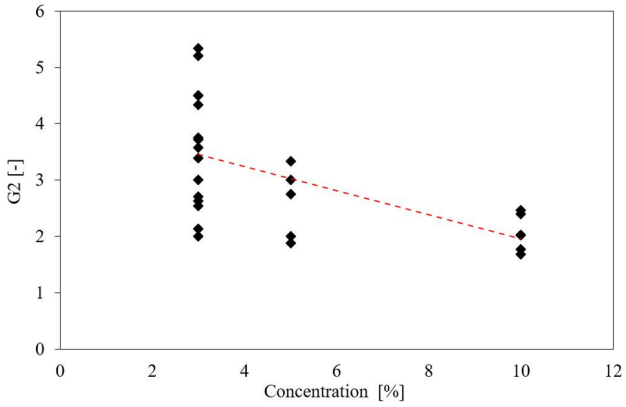

Figure 2.21: Concentration effect on the efficiency of HFMI treatment (simultaneous fatigue-corrosion tests)

$$G1 = \frac{N_{HFMI,Corroded}}{N_{HFMI,New}} \tag{2.6}$$

$$G2 = \frac{N_{HFMI,Corroded}}{N_{AW,Corroded}} \tag{2.7}$$

The fatigue lives of the uncorroded HFMI-treated details are not described in most of the articles where simultaneous fatigue-corrosion tests have been carried out. Therefore, another gain factor is defined to be the ratio between the fatigue lives of the corroded fatigue

lives of the treated details to the as-welded details, see Equation 2.7. This factor is plotted against the concentration of the corrosive medium used in the test. An inverse correlation is found also here as shown in Figure 2.21. Unlike G1, G2 is expected to be always larger than 1.0 as it is normalized to the as-welded condition.

Both figures clearly show that the efficiency of HFMI treatment decreases as a result

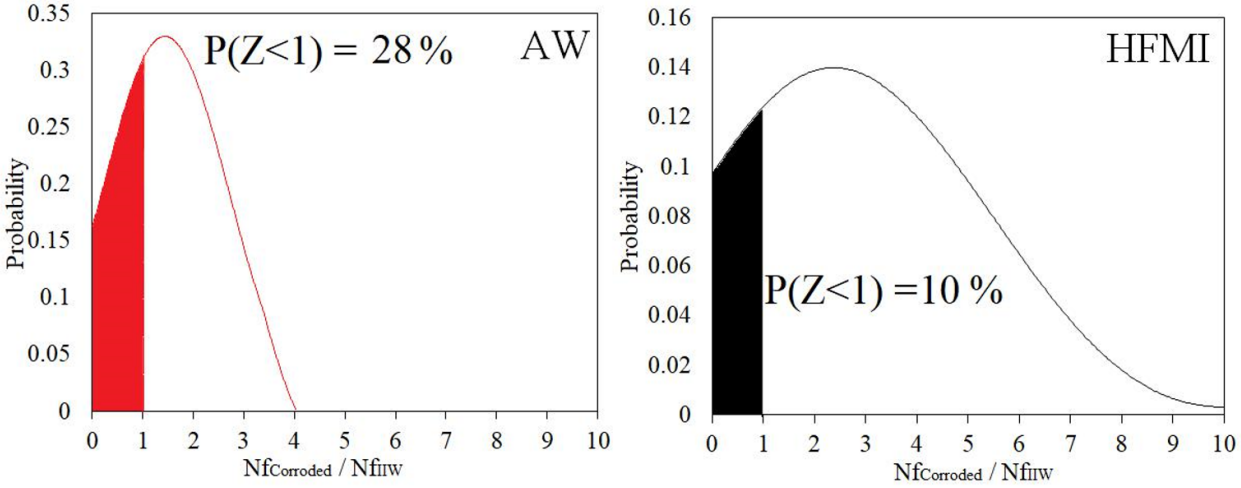

Figure 2.22: Probability density functions of the corrosion fatigue life normalized to the mean recommended fatigue life

of corrosion progression. Nonetheless, it is not yet established that corrosion causes shorter fatigue lives than the design lives assigned by the IIW recommendations [22]. In other words, are the FAT values assigned to HFMI-treated details considered safe even for bridges existing in a corrosive environment? Therefore, the normal distributions of the obtained fatigue lives of corroded specimens (as-welded and HFMI treated) normalized to the mean design lives proposed by the IIW recommendations are plotted for as-welded and HFMI treated details in Figure 2.22. The areas under the curves at which the obtained lives of corroded specimens are less than the mean design values Nf_{IIW} are shaded (for both as-welded and HFMI state). It should be noticed that the mean value of Nf_{IIW} used for the normalization is not the value used in the design as it corresponds to 50% probability of survival, while the design should be made using the characteristic fatigue life which corresponds to 95% probability of survival. In fact, the risk of failing to reach the design life proposed for HFMI-treated details does not exceed 4 % in the studied pool. This is despite the absence of corrosion protection in the conducted fatigue tests.

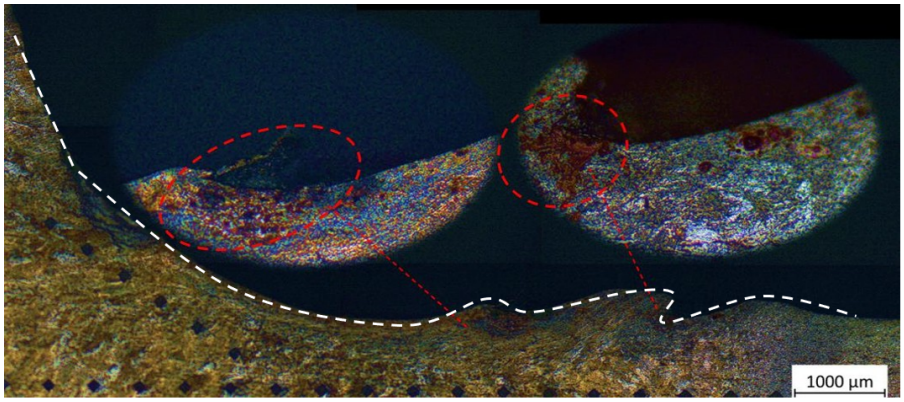

Figure 2.23: Sharp edges after HFMI treatment leads to corrosion

Despite the promising results of HFMI treatment in presence of corrosion, painting

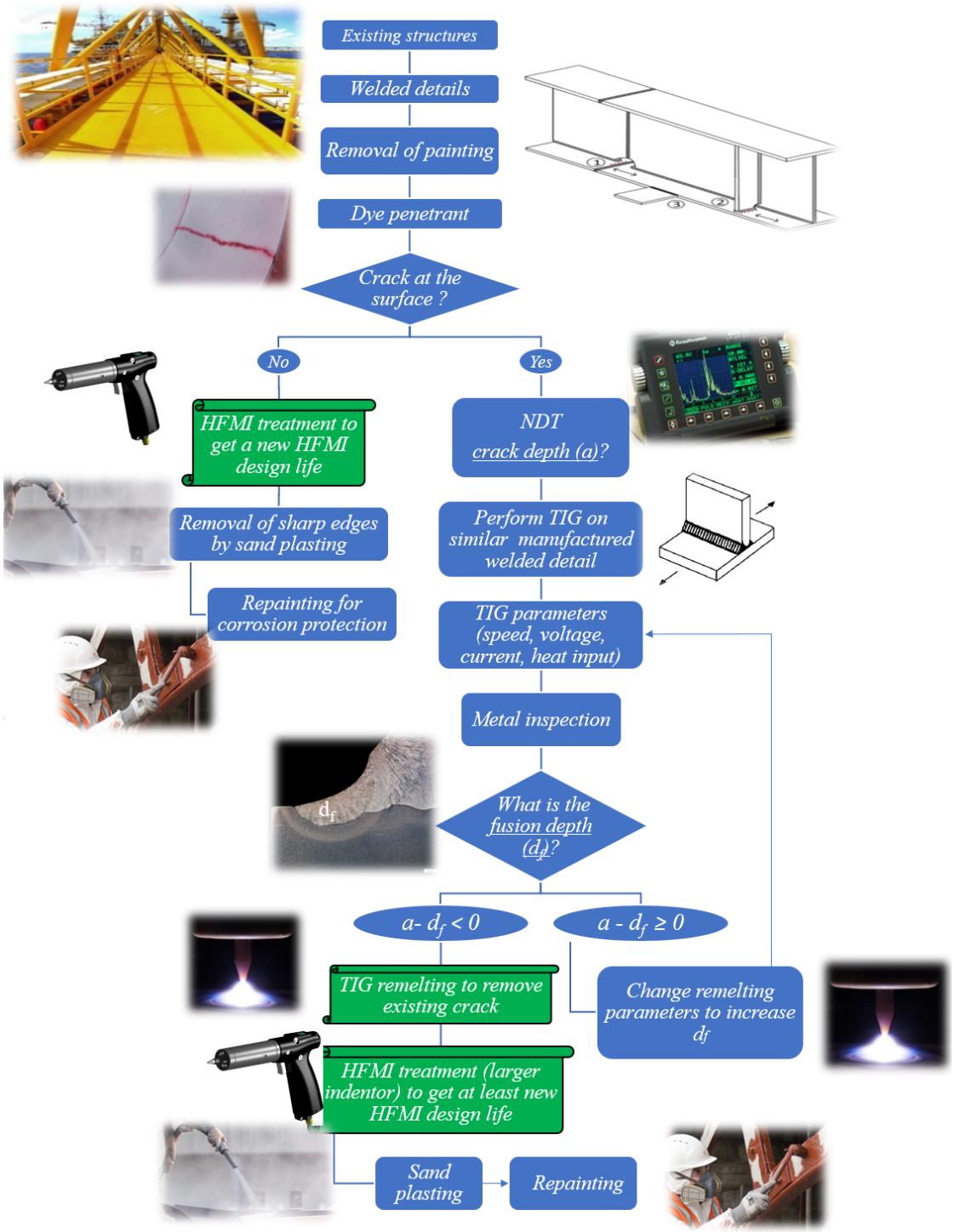

Figure 2.24: Flowchart of the fatigue life extension of existing structures via HFMI treatment

(corrosion protection) should still be applied to reduce the exposure and to utilize the treatment efficiently. Besides, the weld should be visually inspected after HFMI treatment to check the smoothness of the surface, especially at the groove edges. These can be critical locations because dirt and condensed moisture can be trapped which leads to accelerating corrosion. In addition, any sharp edges or corners should be grounded, see Figure 2.23. The grinding should be light in order not to affect the induced compressive

residual stress. Besides, if HFMI treatment is to be applied to an existing structure, non-destructive testing is required to check fatigue cracks as they are also potential locations for dirt and condensed moisture accumulation which leads to ductility reduction in the crack vicinity.

Based on the results presented in this section, practical guidelines for HFMI treatment application on existing bridges are presented in the flowchart given in Figure 2.24. Firstly, the paint layer shall be removed to prepare the weldments for crack detection and HFMI treatment. Afterwards, non-destructive testing should be applied to detect any possible cracks on the surface. If the surface is found to be crack-free, HFMI treatment can then be applied, and a design life longer than the fatigue life of the characteristic new HFMI-treated detail can be claimed. If surface cracks are detected at the toe, HFMI treatment is not recommended unless preceded by TIG remelting if it can ensure the total removal of these cracks. The selection of TIG parameters should be made in a way to achieve a fusion depth larger than the crack size [20]. This includes the speed of remelting, the voltage and the current. In all cases, HFMI treatment shall be followed by light grinding to remove any HFMI sharp groove edges which promote corrosion as stated previously.

3 Design aspects of HFMI treated weldments in steel bridges

The previous chapter clearly shows that HFMI treatment has great potential in enhancing the fatigue performance of existing welded structures, including steel bridges. Therefore, the existing structures can also benefit from fatigue strength improvement assigned by the IIW recommendations. Figure 3.1 shows the improved fatigue strength curves (fatigue strength ranging from 80 to 140 MPa), with the corresponding curves for as-welded details adopted from the Eurocode [8]. It can be noticed that the IIW curves do not differ from the Eurocode curves in only the fatigue strength (i.e. FAT value), but also in different aspects. First, the slopes of the SN curve are changed from 3 & 5 to 5 & 9 above and below the knee point respectively. Besides, the knee point corresponds to 10 million cycles instead of 5 million in the Eurocode curves. Besides, unlike the Eurocode curves, no cut-off limits are assigned in the IIW curves [8].

The level of increase in fatigue strength is dependent on several parameters as stated

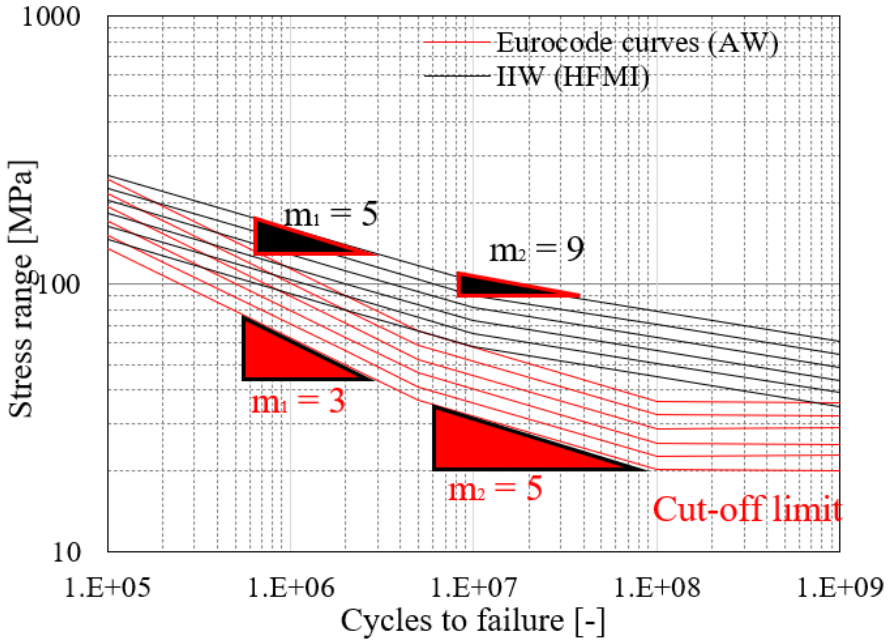

Figure 3.1: The Eurocode 3 version of as-welded fatigue strength curves, compared to those for HFMI treatment (black curves), and the corresponding curves after HFMI treatment (red curves) for $f_y \leq 355$ MPa & R = 0.1

before. Firstly, unlike as-welded details, a direct correlation between fatigue strength increase, and the yield strength of the material, see Figure 3.2. This allows better utilization of high-strength steel which leads to a more lightweight design [75]. Besides, loading conditions might have a considerable negative effect on the fatigue strength of HFMI-treated joints. This is not the case for as-welded details as high tensile residual stresses are assumed to already exist locally at the weld toe [76].

Since HFMI treatment is mainly reliant on the introduced compressive residual stresses, the stability of these stresses is important to be secured throughout the design life of the treated bridge. Therefore, loading conditions that may cause residual stress reduction, or elimination need to be identified and incorporated into design recommendations. At the same time, the verification should be simplified to be used by bridge designers. For example, loading cycles with high mean stresses cause a relaxation of the beneficial introduced compressive residual stresses, which makes the subsequent load cycles more damaging. Besides, overloads with high maximum stress values cause also residual stress relaxation [77].

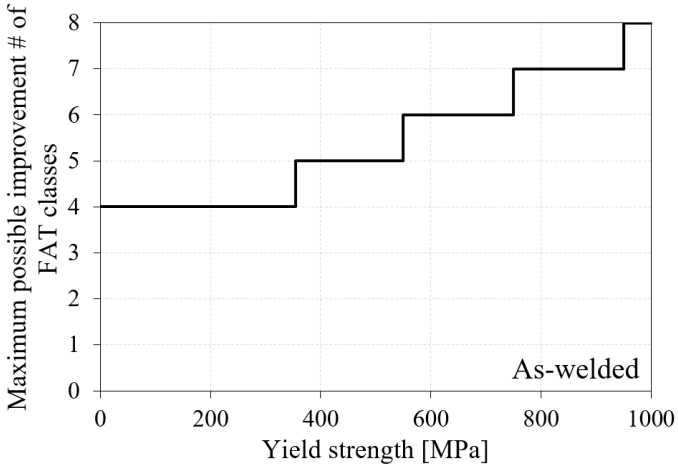

Figure 3.2: Maximum increase in the number of FAT classes as a function of f_y (adopted from [22])

3.1 Stress ratio effect

HFMI treatment is not recommended to be used for loading cycles with stress ratios greater than 0.52 unless the fatigue strength is evaluated using test results [22]. Moreover, the stress ratio effect is expressed as a reduction in fatigue strength class as given in Table 3.1. Besides, a previous publication by Shams-Hakimi suggested a reduction factor to account for the stress ratios expressed in Equation 3.1. This equation is derived from the step-wise decrease proposed by the IIW. This consideration of the R-ratio effect is simple but only applicable to structures subjected to constant amplitude loading with a defined stress ratio. However, bridges are subjected to different types of traffic with different axle loads and configurations. This produces different load cycles with different stress ratios and stress ranges. In addition, traffic loads are usually unknown to engineers in the design phase.

Table 3.1: Stress ratio effect on fatigue strength class [22]

Stress ratio	FAT class reduction
R<0.15	0
0.15<R<0.28	1
0.28<R<0.40	2
0.4<R <0.52	3
0.52<R	No available data

$$f = 0.5R^2 + 0.95R + 0.9 \qquad , f_i \geq 1.0 \tag{3.1}$$

A detailed study of the in-service stresses in road bridges showed that some weldments are subjected to load cycles with high-stress ratios up to 0.9 due to real traffic. [5]. This is beyond the penalty method presented in Table 3.1. Nonetheless, several research articles have investigated the effect of HFMI treatment on the fatigue strength of welded details subjected to high R-ratios [32–35, 78–80]. For instance, four strength class reduction is proposed for R-ratios greater than 0.5 [34], and more fatigue tests were conducted under relatively high-stress ratios, and the results supported the trend of the IIW method. The trend follows a decrease of one fatigue strength class per 0.12 increase in the stress ratio. Therefore, this trend is proposed for higher R ratios up to R $\approx$ 1. It should be noticed that the self-weight of the bridge might cause increased mean stress which thereby increases the stress ratio in the HFMI-treated welded details in the bridges. This is, for instance, the case if the treatment is performed before bridge erection (i.e. the application of the self-weight). On the other hand, if the treatment is performed after bridge erection (e.g. such as treating an existing structure), the compressive residual stress induced by HFMI treatment is not expected to affect the self-weight [19, 57].

A design method to consider the stress ratio effect due to both the bridge self-weight and the variation of real traffic load was developed in [81]. This method can be used in conjunction with the load models in Eurocode and does not require prior knowledge of the traffic load. In this method, the severity of the mean stress (i.e. the stress ratio) effect is considered in one factor, λ_{HFMI} which is used to magnify the design stress range accounting for the variation of mean stress from self-weight and from the passage of real traffic over the bridge. Expressions of λ_{HFMI} for road bridges which were proposed in [76] are given in Equations 3.2 & 3.3 for mid-span and mid-support sections respectively. The mid-support section is defined within 0.15L from the intermediate support, and the mid-span section is assumed elsewhere. Φ in these equations takes the effect of self-weight stress into account. These equations were derived using a limited traffic sample size of 55,000 measured lorries in Sweden. Therefore, they need to be validated for use on road bridges using more measured vehicle data from Sweden and elsewhere. Besides, similar equations need to be derived for railway bridges to account for the mean stress effect.

$$\lambda_{HFMI} = \frac{2.38\Phi + 0.64}{\Phi + 0.66} \qquad \lambda_{HFMI} \geq 1 \quad \text{For the Mid-Span} \tag{3.2}$$

$$\lambda_{HFMI} = \frac{2.38\Phi + 0.06}{\Phi + 0.40} \qquad \lambda_{HFMI} \geq 1 \quad \text{For the Mid-Support} \tag{3.3}$$

3.1.1 Traffic measurements

Traffic data measured from Sweden and the Netherlands have been provided including hundreds of thousands of trucks. The provided data includes the axle loads, the axle spacing and the number of axles. The data were measured using the weight in motion method [82, 83]. In addition, the original data used to derive the method is also included in the analysis. The weight-length distributions of the different studied traffic data are shown in Figure 3.3. The number of lorries in each data pool is given in Table 3.2. In addition, 220 trains were measured in Sweden to investigate the mean stress effect in railway bridges. The cumulative distributions of the axle load and the axle distance of the studied data pool are given in Figure 3.4.

Table 3.2: Number of lorries in each data pool $x10^3$

Number of axles	Original data [5]	Extended Swedish data [83]	Dutch data 2008 [82]	Dutch data 2018 [82]
2-axles vehicles	8	173	29	21
3-axles vehicles	7	109	15	14
4-axles vehicles	4	80	58	56
5-axles vehicles	13	189	120	112
6-axles vehicles	8	110	14	15
7-axles vehicles	13	179	1	2
8 or 9-axles vehicles	2	33	1	1
Total	55	873	238	221

3.1.2 Framework for predicting the mean stress effect

The measured vehicles are transported along several influence lines for simply supported and continuous bridges. This includes the measured vehicles from different data pools and the measured train data from Sweden. Then, the mean stress (i.e. the stress ratio) effect is expressed as the ratio between the equivalent stress range adjusted using the modification factor (f) for each loading cycle, to the un-adjusted one as given in Equations 3.4, 3.5 & 3.6. The contribution of the bridge self-weight is given in Φ which is normalized to the maximum stress range generated by the traffic as shown in Equation 3.7. An obvious relationship is found between Φ & λ_{HFMI} for all influence lines, which includes several

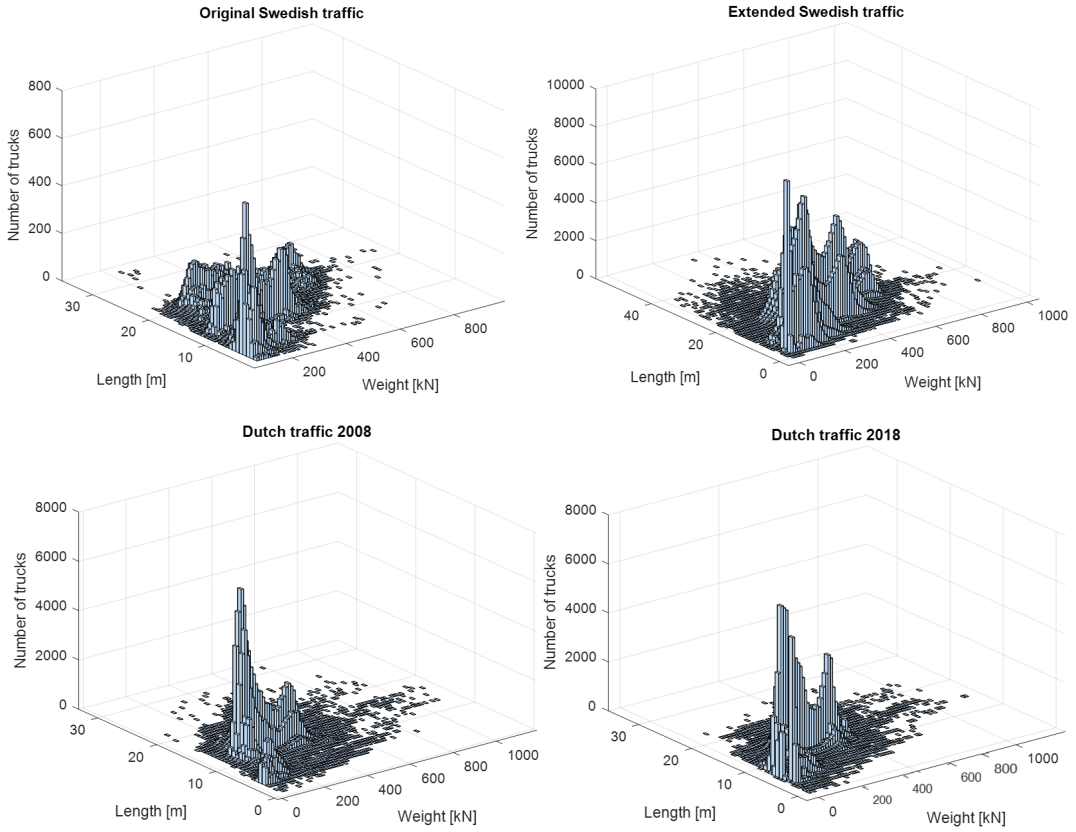

Figure 3.3: Weight-length distributions for the different studied traffic

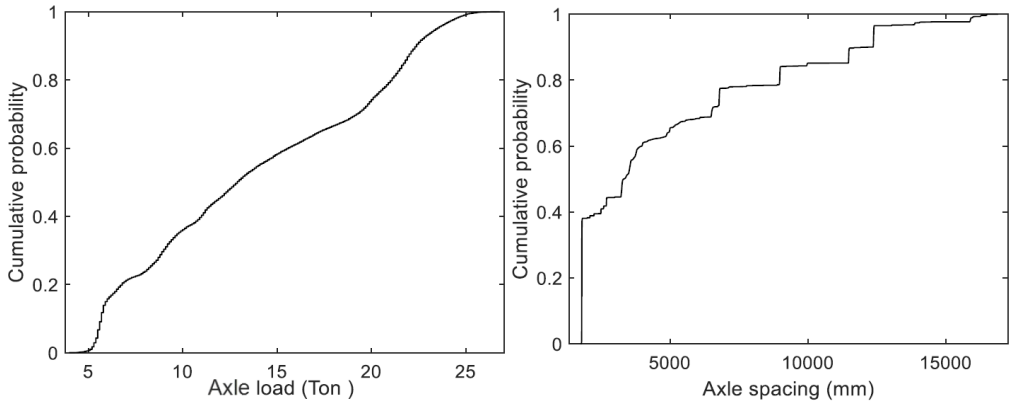

Figure 3.4: Axle load and axle distance distributions of the measured trains

beam locations from the mid-span to over the support.

The validity of equations 3.2 & 3.3 in representing the mean stress effect is examined by comparing the generated $\Phi - \lambda_{HFMI}$ curves for the original data pool (used for deriving the method), to the studied extended data pools. The comparison is made with respect to the shortest span length in both the simply supported and continuous beams since they were proposed for design [81]. Upon comparison shown in Figure 3.5, the named equations are considered to be safe which validates their use to account for the mean stress (i.e. stress ratio) effect in road bridges.

For train traffic, the different generated $\Phi - \lambda_{HFMI}$ are plotted in Figure 3.6. These curves correspond to different influence lines and different span lengths. The upper bound

curve corresponds to the mid-span location of the simply supported bridge with L = 10 m, whereas the lower bound corresponds to the mid-support location of the continuous bridge with L = 100 m. For simplicity, the highest curves corresponding to the mid-span section (0.5L, simply supported), and the mid-support section (0.85L, Continuous) are proposed for design purposes. The fitted expressions of these two curves are given in Equations 3.8 & 3.9.

$$\Delta\sigma_{EQV} = \sqrt[m]{\frac{\Sigma(n_i.\Delta S_i)^m)}{\Sigma n_i}} \tag{3.4}$$

$$\Delta\sigma_{EQV,R} = \sqrt[m]{\frac{\Sigma(n_i.(\Delta S_i.f_i)^m)}{\Sigma n_i}} \tag{3.5}$$

$$\lambda_{HFMI} = \frac{\Delta\sigma_{EQV,R}}{\Delta\sigma_{EQV}} \tag{3.6}$$

$$\Phi = \frac{S_{SW}}{\Delta S_{max}} \tag{3.7}$$

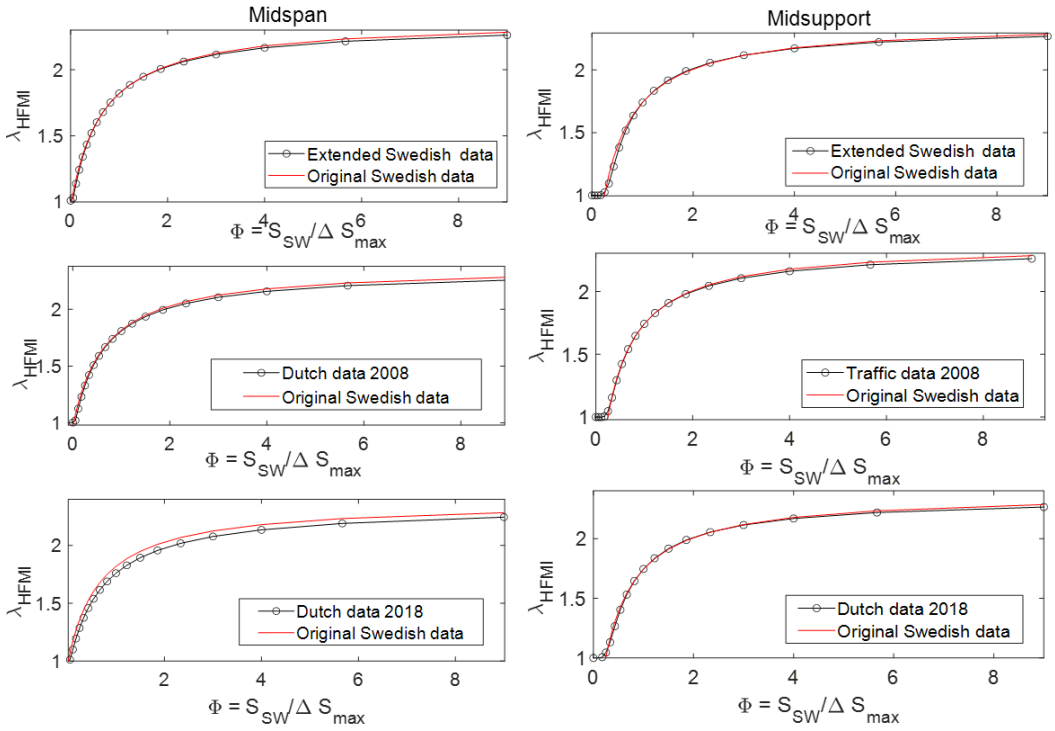

Figure 3.5: Comparison of $\Phi - \lambda_{HFMI}$ curves calculated using the studied traffic and Equations 3.2 and 3.3 for the mid-span and mid-support sections, respectively.

$$\lambda_{HFMI} = \frac{2.375\Phi + 1.183}{\Phi + 1.074} \qquad \lambda_{HFMI} \geq 1 \quad \text{For the Mid-Span} \tag{3.8}$$

$$\lambda_{HFMI} = \frac{2.564\Phi + 1.116}{\Phi + 1.608} \qquad \lambda_{HFMI} \geq 1 \quad \text{For the Mid-Support} \tag{3.9}$$

ΔS_{max} (which is needed to calculate Φ & λ_{HFMI}) is seldom available for bridge designers as future traffic is not known. Therefore, a practical method to obtain ΔS_{max} is proposed by constructing a relationship between ΔS_{max} to another parameter easy to obtain by designers. For road bridges, the stress range generated by the fatigue load model

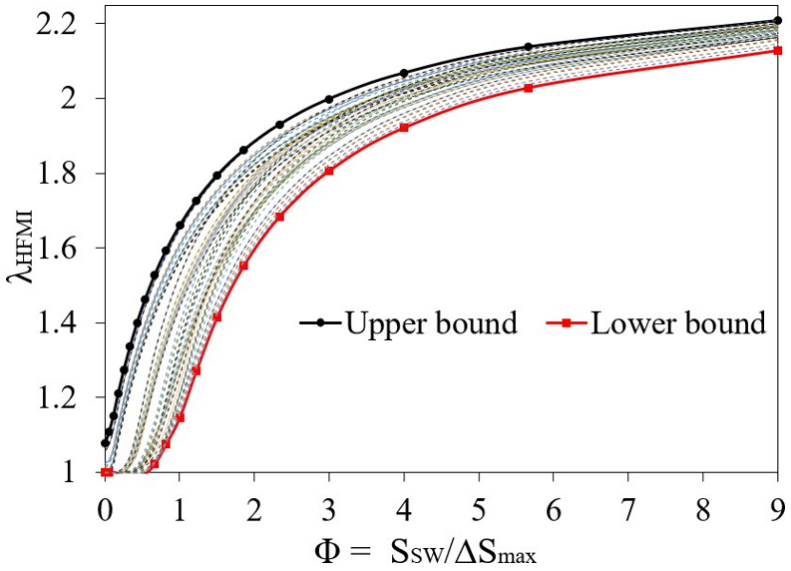

Figure 3.6: All generated $\Phi - \lambda_{HFMI}$ curves for railway bridges

3, ΔS_P is considered as an alternative in calculating Φ. Based on the conducted analyses an approximation of $\Delta S_{max} = 2\Delta S_P$ is proposed [81]. Likewise, a relationship is suggested between ΔS_{max} and the stress range generated by either load model, LM71 or the maximum stress range generated due to the passage of the trains consisting of the different mixes in Eurocode [84]. Therefore, ΔS_{max} is approximated to be $0.73\Delta S_{LM71}$ or $0.9\Delta S_{max,mix}$ depending on the used fatigue verification method (λ-coefficient or damage accumulation method).

3.1.3 Comparison to load models

For fatigue design or verification, the stress ranges are calculated using traffic load models. FLM3 & FLM4 are some of the models used for fatigue verification for road bridges, while LM71 and different train mixes are used for railway bridges. [84]. The mean stress effect can not be predicted using the stress ratios generated by these models unless they are validated against real measured traffic. Therefore, λ_{HFMI} is calculated and compared via real traffic and load models for road and railway bridges in Figure 3.7 & 3.8 respectively. Both plots give the highest obtained $\Phi - \lambda_{HFMI}$ curves which correspond to a short span in the simply supported beam as stated earlier.

It can be noticed that the fatigue load models used in conjunction with the λ-coefficients methods such as LM71 in railway bridges, or FLM3 in road bridges underestimate the mean stress effect significantly. This is because the load considered in these models are quite heavy [10]. On the other hand, the more complex models such as FLM4 (which consists of 5 standard trucks), or train mix (which consists of 12 trains) give a better representation of the real mean stress effect. Nonetheless, only light traffic composition may result in a close prediction of the mean stress effect collectively. This includes light train mix and local composition in FLM4.

All load models (except those with light compositions) are heavier than the measured real traffic. Heavier traffic generates cycles with a larger stress range but with lower mean stress as the stress ratios of such cycles are smaller than those of cycles with a lower stress range. This explanation may be used also to understand why Swedish traffic produces higher mean stress than Dutch traffic as shown in Figure 3.5. The Dutch traffic data pools include some exceptional heavy vehicles (which require special permits) which is not the case in the Swedish filtered data [82]. Based on this, the different studied fatigue load models are found to be inappropriate to incorporate the mean stress effect in fatigue

design directly. This makes the proposed equations necessary to account for the mean stress effect. A special case is identified for bridges that are designed to carry the same type of train for their whole design life such as 'Malmbanan' in the north of Sweden. Equations 3.8 & 3.9 are derived using various types of trains which makes them not applicable for single-typed traffic. In this case, the mean stress can be directly incorporated by magnifying the generated loading cycles due to the passage of the used load model (such as local model 13S in Sweden [85]). The magnification factor f given in Equation 3.1 (which is derived from the penalty factor proposed by the IIW recommendations) can be used to account for the mean stress effect in this case.

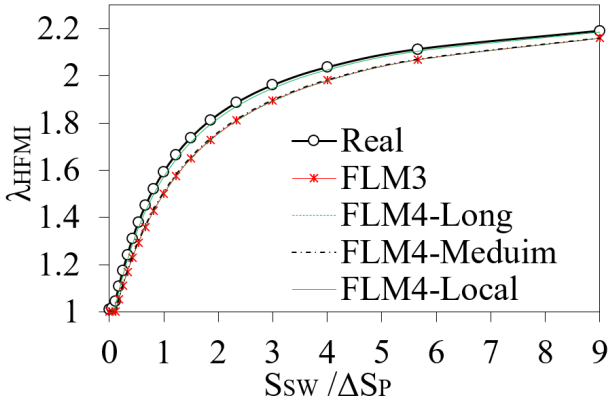

Figure 3.7: Comparison between $\Phi - \lambda_{HFMI}$ curves for fatigue load models and measured trucks

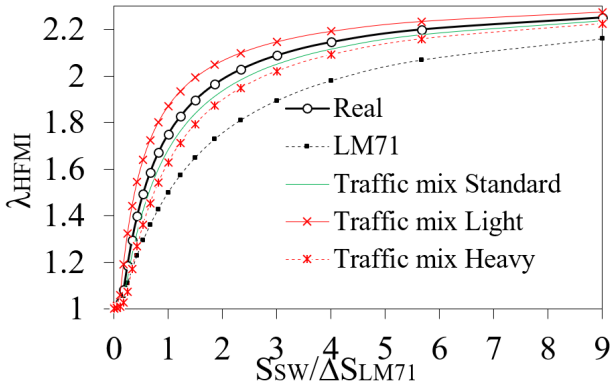

Figure 3.8: Comparison between $\Phi - \lambda_{HFMI}$ curves for fatigue load models and measured trains

3.2 Maximum permissible stresses

Previous research has demonstrated the harmful effect of overloads on the compressive residual stress induced by HFMI treatment [77, 86, 87]. Besides, compressive overloads are verified to be more harmful than tensile ones. This is because when superimposing high compression with the existing compressive residual stress induced by HFMI treatment, local yielding occurs at a lower value compared to the case where the imposed load is tensile. Therefore, it is not recommended to use HFMI treatment to enhance welded details subjected to loading cycles with a maximum compressive stress of $0.8f_y$ [22, 88]. However, the incorporation of this in design and assessment of HFMI-treated weldments in steel bridges is still unclear. In order to do this, the annual maximum stresses carried by the bridge need to be identified.

3.2.1 Statistical analysis of the extreme traffic loads

For traffic action, the load is defined by its characteristic value which is usually the 98th percentile of the annual maximum distribution equivalent to a 50-years return period of the bridge design [89]. One goal is to characterize the maximum load effect (i.e. bending moment) during the reference period. Therefore, extreme value analyses are conducted using the real measured traffic in Sweden and Netherlands. Gumbel distribution is an extreme value distribution that can describe the maximum bending moment induced by vehicles in highway bridges [89]. The random variable is assigned to be the maximum bending moment generated by the passage of each measured truck on the studied influence lines.

Determining Gumbel distribution parameters directly is difficult as the available traffic data are limited. Therefore, statistical extrapolation is required. The peak over threshold (POT) method is used to determine Gumbel distribution parameters using the available data. The maximum obtained bending moments are divided into blocks, each block representing one measurement day. The maximum generated bending moment in each block

is then chosen as shown in Figure 3.9. Afterwards, a threshold is selected, and the data above the threshold is fitted to an exponential distribution. The process of selecting the threshold is iterative until the quality of fitting becomes satisfactory. Afterwards, the intensity of vehicles generating bending moments above the threshold is determined for a selected reference period of one year. Then, the selected threshold (u), the intensity of exceedance (λ) and the exponential distribution parameter (m) are used for determining the Gumbel distribution as expressed in Equation 3.10. The characteristic value is then evaluated to be the 98th percentile of the obtained distribution. Figure 3.10 shows an example of the resulting cumulative distribution function. The figure clearly indicates that the obtained distribution gives moments larger than the empirical distribution of the data, and its daily maxima. Besides, the figure also demonstrates the quality of the exponential distribution fitting to the moment values above the threshold.

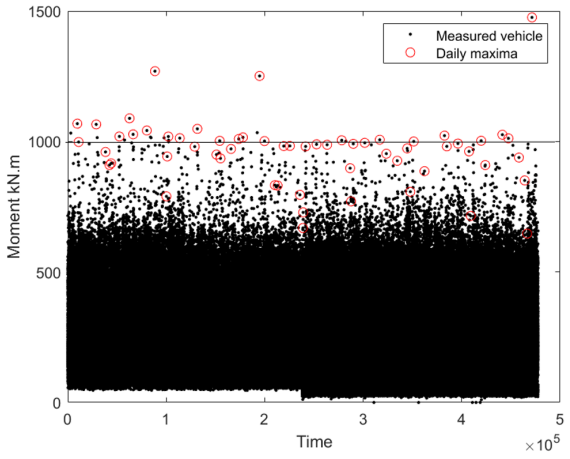

Figure 3.9: Extraction of the daily maxima, with an assumed threshold of M = 1000 kN.m

$$F(x) = e^{-e^{\frac{-(x-u-\ln\lambda)}{m}}} \tag{3.10}$$

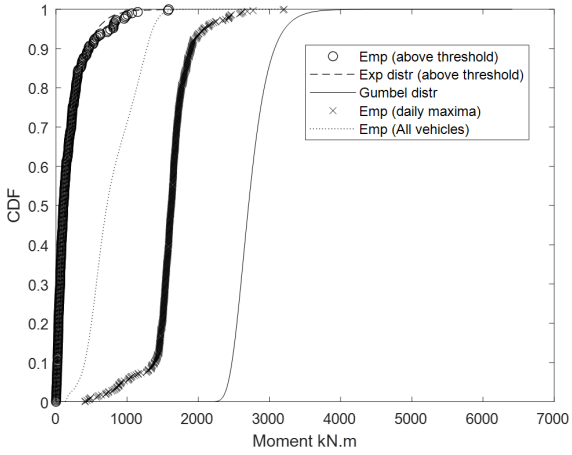

Figure 3.10: An example of the cumulative distribution function of Gumbel distribution

3.2.2 Comparison to load model

The loads considered in the design of composite road bridges include permanent loads, traffic loads, climate loads such as thermal and wind loads, and internal loads due to concrete creep and shrinkage. The largest uncertainty in the load model corresponds to the

Table 3.3: Multipliers used for different combinations

State	Ultimate limit state	Serviceability limit state	
	-	Frequent combination	Characteristic combination
γ_Q	1.5	1.0	1.0
Ψ_0	1.0	0.75 (Point load), 0.4 (Distributed)	1.0

environmental and traffic loads. However, traffic load has a more prominent influence on the design [90]. This makes the uncertainty related to traffic more influential. Besides, the uncertainty in the load model for permanent load is smaller than the traffic load. Therefore, toward the aim of identifying the maximum annual stresses carried by the bridge, the load effects generated by the traffic load model (such as load model 1) are compared to those generated by real measured traffic obtained using POT method.

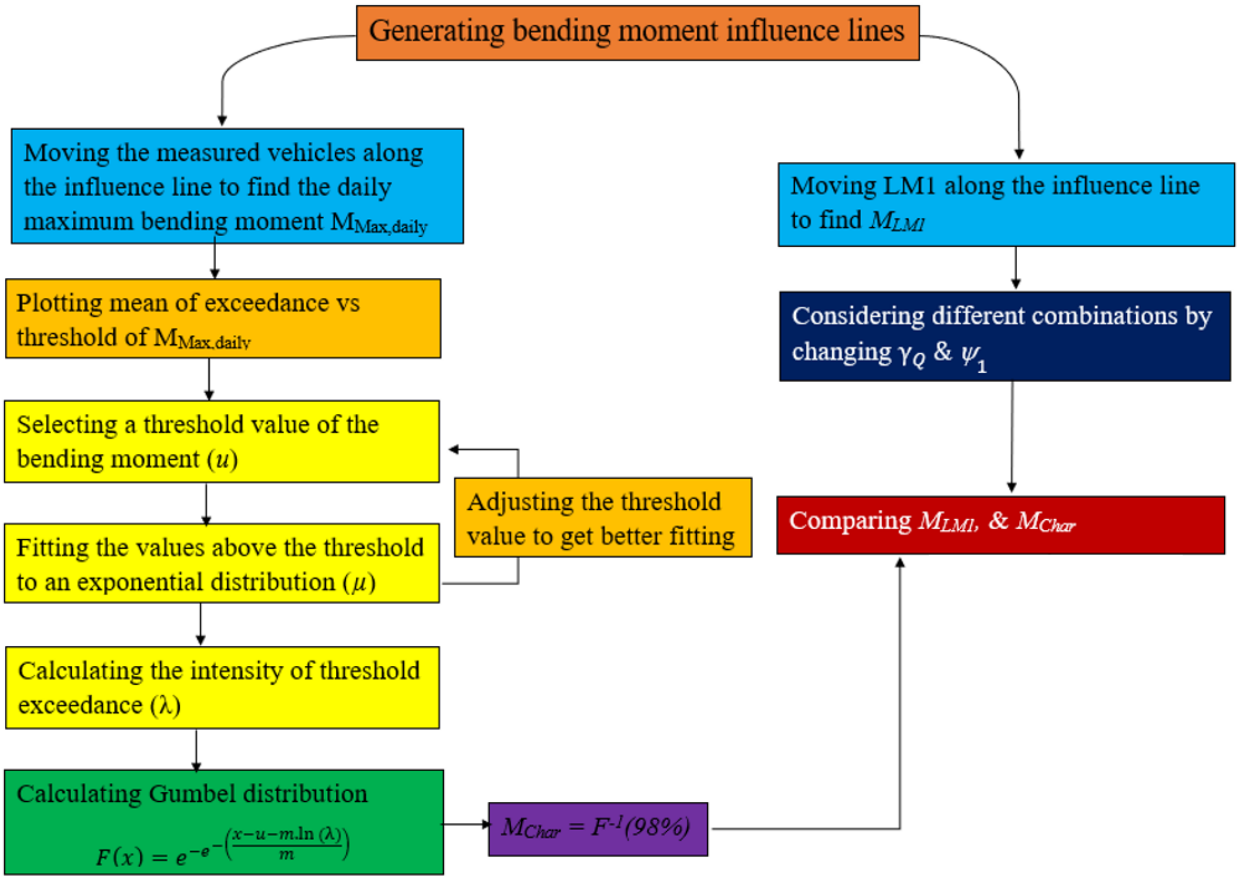

Figure 3.11: Flowchart for the maximum permissible stress identification

Load model 1 is one of the most widely used models to represent traffic load in the design of road bridges in both ultimate limit state, and serviceability limit states [91]. However, different factors and multipliers are used for different limit state conditions, as given in Table 3.3. It should be noticed that this load model produces different load effects for a different number of lanes. Herein, two lanes are considered. Figure 3.11 summarizes the procedures of obtaining the characteristic values of bending moment via the POT method and comparing them to those obtained by LM1 considering different combinations. The comparison is shown in Figure 3.12 for different span lengths and positions along the beams (from the midspan to the support).

The shown results clearly indicate that the ultimate limit state load significantly over-

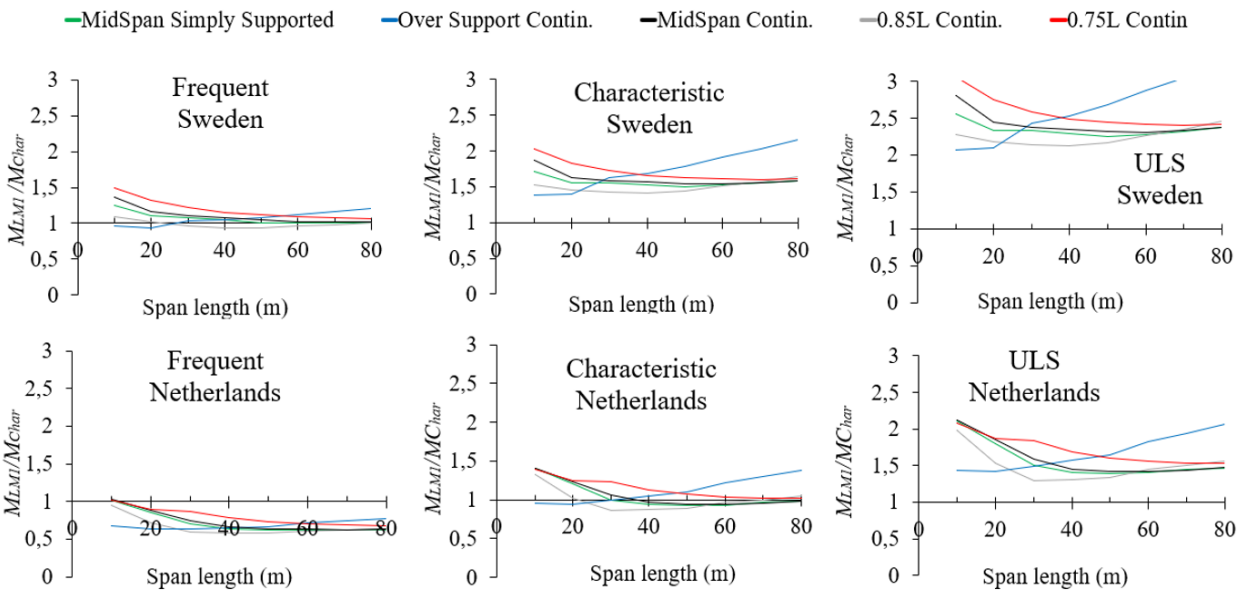

Figure 3.12: Comparison of LM1 in different combinations versus real traffic

estimate the real loads (estimated statistically) in both Sweden and the Netherlands. On the other hand, the frequent combination underestimates it in the Netherlands, while the characteristic combination appears to be the best-studied option. The difference between the two countries might be explained by the exceptional transport with heavy vehicles in the Netherlands as mentioned before [82]. Therefore, the characteristic combination is found to be the most appropriate for verifying HFMI-treated details in road bridges.

Railway bridges are expected less likely to be subjected to the same type of overloads as is the case for road bridges. Therefore, the characteristic combination is expected to be sufficient to check the maximum allowable stresses in HFMI-treated details. Nonetheless, this could not be verified without further research.

3.3 Design examples

Fatigue verification of welded details is performed and presented in this section to illustrate how the different aforementioned effects can be incorporated into the design or assessment of HFMI-treated welded details in road and railway bridges. One structural detail (i.e. non-load carrying transverse attachment) is studied in the mid-span in both bridges. Information about the studied bridges and the considered constructional details are given in Table 3.4. The fatigue assessment is made via either the λ-coefficients or damage accumulation methods. The cross-section and the elevation view of the bridges are shown in Figure 3.13.

Six and five increments in FAT class can be assigned to a transverse attachment made of S690 (assumed for road bridge), and S355 (assumed for railway bridge) respectively [22]. This elevates the fatigue strength of as-welded detail from 80 MPa to 160 & 140 MPa respectively. Besides, a thickness reduction factor of $(25/t)^{0.2}$ is to be applied for plate thickness exceeding 25 mm according to the IIW recommendations [22]. This explains the lower FAT value in the second case study given in Table 3.4. Another reduction factor can be applied to take the stress ratio effect into account as given in Equation 3.1. However, this is not applicable as the bridges are subjected to variable amplitude loading.

$$\Delta\sigma_E = \lambda \times \lambda_{HFMI} \times \Delta\sigma_{LM} \times \gamma_{Ff} \tag{3.11}$$

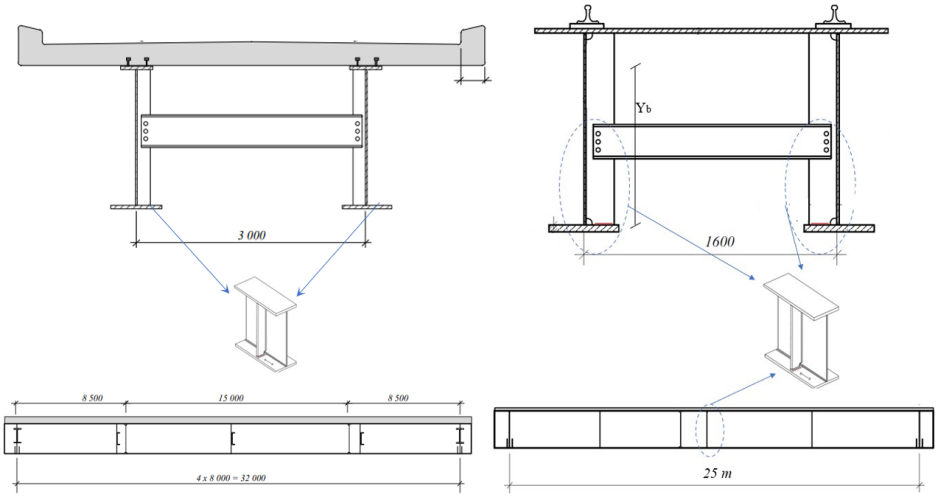

Figure 3.13: Cross-section and elevation views of the studied road and railway bridges

Table 3.4: Information about the studied case study bridges, with the studied constructional details

Case study 1: Composite road bridge			
Span length	Design life	Section modulus	Distribution factor
L (m)	t (year)	W (mm^3)	LDF (-)
32	80	3.876×10^7	0.833
Traffic volume	Traffic category	Concrete slab class	Steel grade
50000	4	C35/45	S690
Position	Fatigue strength	Self-weight	Lorry weight
x (m)	FAT (MPa)	$S_{SW}(MPa)$	Q_{Obs} (kN)
16	160	120	310
Case study 2 : Railway bridge			
Span length	Design life	Section modulus	Dynamic amplification
L (m)	t (year)	W (mm^3)	$\phi(-)$
25	120	8.023×10^7	1.157
Steel grade	Fatigue strength	Position	Self-weight stress
(-)	FAT (MPa)	x (m)	$S_{SW}(MPa)$
S355	118	12.5	10.8

$$N_f = 10^7 \times \left(\frac{\Delta\sigma_{D,HFMI}}{\Delta\sigma_{EQV} \times \gamma_{Ff} \times \lambda_{HFMI}}\right)^{m_1,m_2} \tag{3.12}$$

The stress ratio (i.e. mean stress) effect is to be considered via magnifying the stress range calculated from load model FLM3, or LM71 in the λ-coefficient method as given in Equation 3.11. The different λ-coefficients needed for calculating the $\Delta\sigma_E$ are given in Table 3.5. In the damage accumulation method, λ_{HFMI} is used to magnify the equivalent stress range $\Delta\sigma_{EQV}$ as given in Equation 3.12. $\Delta\sigma_{EQV}$ is calculated in Equation 3.13. Table 3.6 gives the different number of lorries and the calculated stress ranges (in local traffic in FLM4), and trains (in light traffic mix). The fatigue damage is then calculated via Equation 3.14 or 3.15 depending on the fatigue assessment method. The results of fatigue damage calculations are given in Table 3.7.

Table 3.5: The different λ values needed for the λ-coefficient method

Case study 1: Composite road bridge					
λ_1	λ_2	λ_3	λ_4	λ_{max}	λ
2.33	0.407	0.956	1	2	0.907
Case study 2 : Railway bridge					
λ_1	λ_2	λ_3	λ_4	λ_{max}	λ
0.65	1.0	1.04	1.0	1.38	1.36

Table 3.6: Train/lorries considered for the damage accumulation method

Case study 1: Composite road bridge						
Lorry number	1	2	3	4	5	
lorry/Year	40,000	2500	2500	2500	2500	Total = 50,000
$\Delta\sigma$ (MPa)	31	48	66	51	57	$\Delta\sigma_{EQV}$ = 49
Case study 2 : Railway bridge						
Train number	1	2	5	9		
train/Year	3650	1825	730	69350		Total = 75555
$\Delta\sigma$ (MPa)	54	41	71	25		$\Delta\sigma_{EQV}$ = 44

$$\Delta\sigma_{EQV} = \begin{cases} \sqrt[m_1]{\dfrac{\sum(n_i\Delta\sigma_i^{m_1}) + (\dfrac{\Delta\sigma_{D,HFMI}}{\gamma_{M,f}})^{m_1-m_2} \times \sum(n_j\Delta\sigma_j^{m_2})}{\sum(n_i+n_j)}} & , \dfrac{\Delta\sigma_{D,HFMI}}{\gamma_{M,f}} > \Delta\sigma_{EQV} \\ \sqrt[m_2]{\dfrac{\sum(n_i\Delta\sigma_i^{m_1}) \times (\dfrac{\Delta\sigma_{D,HFMI}}{\gamma_{M,f}})^{m_2-m_1} + \sum(n_j\Delta\sigma_j^{m_2})}{\sum(n_i+n_j)}} & , \dfrac{\Delta\sigma_{D,HFMI}}{\gamma_{M,f}} \leq \Delta S_{EQV} \end{cases} \tag{3.13}$$

$$D = (\frac{\Delta\sigma_E}{FAT/\gamma_{Mf}})^{m_1} \tag{3.14}$$

$$D = \frac{\sum n_i + \sum n_j}{N_f} \tag{3.15}$$

Some railway bridges are designed to transport the same type of train for the whole design life. In this case, special load models shall be used such as model 13S which is proposed by the Swedish transport administration for some railway lines in Sweden carrying one train type consisting of Fanno-type wagons [85]. If this is the case, the mean stress is to be incorporated directly via magnifying the stress ranges with the factor f expressed in Equation 3.1. Since f depends on the stress ratios, the cycles due to passing

Table 3.7: Fatigue assessment of the studied constructional detail

	Road bridge		Railway bridge	
Method	λ coefficient	Damage accumulation	λ coefficient	damage accumulation
load model	FLM3	FLM4 (regional)	LM71	Traffic mix (light)
Stress range	ΔS_P (Equation 3.11)	$\Delta\sigma_{EQV}$ (Equation 3.13)	$\Delta\sigma_{LM71}$(Equation3.11)	$\Delta\sigma_{EQV}$(Equation 3.13)
	64 MPa	49 MPa	77 MPa	44 MPa
Φ	SW / 2 ΔS_P	SW / 2 ΔS_P	SW / 0.73 $\Delta\sigma_{LM71}$	SW / 0.9 $\Delta\sigma_{max,mix}$
	0.938		0.150	0.168
λ_{HFMI}	(2.38 Φ +0.64)/(Φ +0.66)		(2.375 Φ + 1.183)/(Φ +1.074)	
	1.797	1.797	1.171	1.188
Fatigue damage	Equation 3.14	Equation 3.12 & 3.15	Equation 3.14	Equation 3.12 & 3.15
	0.527	0.194	0.390	0.140

the load over the influence line need to be identified as shown in Figure 3.14. $\Delta\sigma_{EQV}$ is then calculated in Equation 3.16.

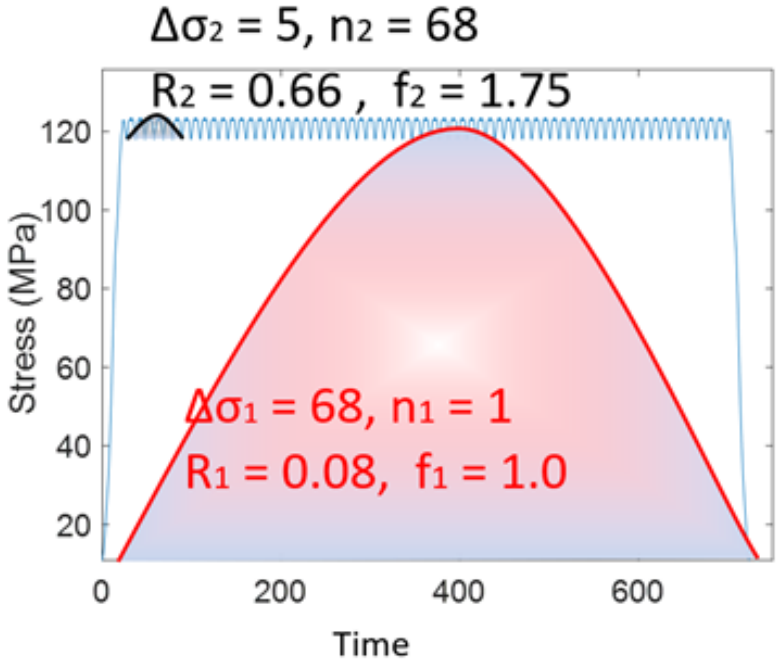

Figure 3.14: The stress response in the welded detail due to the passage of 13S (the characteristics of the generated stress cycles are noted)

$$\Delta\sigma_{EQV} = \sqrt[m_2]{\frac{n_1(\Delta\sigma_1.f_1)^{m_1} \times (\frac{\Delta\sigma_{D,HFMI}}{\gamma_{M,f}})^{m_1-m_2} + n_2(\Delta\sigma_2.f_2)^{m_2}}{n_1+n_2}} = 64.3MPa \tag{3.16}$$

The maximum stresses should be calculated including the static load effects from the characteristic combination of actions as stated earlier. In composite road bridges, the characteristic combination includes the self-weight stress (SW), thermal stress (T_K), stress rises due to concrete shrinkage (S), wind load (F_w) and traffic load. For road bridges, LM1, which consists of both concentrated (TS) and uniformly distributed loads (UDL) are used to represent traffic load. The characteristic stress should not exceed 0.8 f_y as given in equation 3.17. Upon calculations, the characteristic stresses in the mid-span do not exceed $0.45f_y$. Similarly, for the railway bridge, the characteristic stresses are expressed in Equation 3.18.

$$SW + (1 \ \ or \ \ 0) \times S + TS + UDL + 0.6 \times max(F_w, T_k) = 300MPa = 0.45fy \tag{3.17}$$

$$SW + LM71 + 0.6 \times max(F_w, T_k) = 120MPa = 0.34fy \tag{3.18}$$

4 Summary, Concluding remarks & Future work

4.1 Summary and Conclusions

The aim of the research presented in this thesis is to provide rules and recommendations which are needed for the application of HFMI treatment on existing and new road and railway bridges. Within this area, experimental, numerical and analytical work is carried out. Moreover, traffic data analyses are performed, and statistical evaluations are conducted. Based on the studies in this thesis, the following main conclusions can be drawn:

- The effect of HFMI treatment on existing structures containing cracks is studied experimentally and via analysing collected data from the literature. The results verify that HFMI treatment can successfully prolong fatigue endurance significantly to an extent that the fatigue strength assigned for new HFMI-treated details can be claimed. In other words, the FAT values assigned for HFMI-treated weldments can be used for weldments in existing structures. The only condition that needs to be checked is that the existing crack size is not deeper than 2.25 mm. Nonetheless, due to inaccuracy in most of the crack inspection methods, it is recommended to use HFMI treatment only if the inspection reveals no crack at the surface.
- Microscopic investigations have shown that HFMI treatment causes both a decrease in the existing crack width and a change in crack inclination. However, both these effects decay as the crack becomes deeper. Besides, it is recommended that HFMI indentor should be directed more toward the based metal in order to avoid unintentional crack opening -if any exists at the surface-.
- The effect of preceding HFMI treatment with remelting using a tungsten electrode on the fatigue life is studied experimentally and numerically. It is found that this combination gives fatigue life superior to both individual treatments (TIG remelting or HFMI treatment) if they were performed alone. This is explained by the improvement in both the compressive residual stress due to HFMI treatment and the local topography due to remelting. Besides, the available fatigue test results have shown that the weldments after combined treatment become stronger than the base metal. TIG-HFMI combination is found to give a relatively long fatigue life even with the presence of surface, or subsurface cracks no deeper than 4 mm. Nonetheless, due to expenses and complexity associated with the application of TIG remelting on site, it is suggested to use this combination only if the crack inspection reveals crack on the surface, and deeper fusion can be achieved using TIG remelting.
- The effect of corrosion on HFMI treated details is studied via analysing collected fatigue test results. An opposite correlation is found between fatigue endurance and the corrosion level (concentration of the corrosive medium, and the time of exposure). Nonetheless, the risk of obtaining a fatigue life shorter than the design life assigned for treated details does not exceed 4% in the studied pool even when corrosion protection is not applied. For practical applications, it is suggested to remove the sharp groove edges produced by the treatment as they promote corrosion, and to follow HFMI treatment with sand-blasting and corrosion protection.
- The incorporation of stress ratio (i.e. mean stress) effect in HFMI-treated weldments in road and railway bridges subjected to variable amplitude loading is studied in this thesis via analysing measured train and truck data. One parameter λ_{HFMI} is proposed to take the mean stress due to self-weight and traffic variations into account. This parameter is used to magnify the stress range generated by the load model in the λ-coefficients or damage accumulation verification methods. If the treatment is performed after bridge erection, the self-weight stress effect on the mean stress can be ignored.
- the accuracy of mean stress effect predictions via Eurocode's fatigue load models is investigated. It is found that the load models associated with the λ-coefficients methods such as FLM3 in road bridges, or LM71, SW/0 and SW/2 in railway bridges significantly underestimate the mean stress effect. Better prediction of the mean stress

effect is obtained via the models associated with the damage accumulation method but even these lead to underestimation of mean stresses in most cases. Therefore, the use of the proposed modification factor λ_{HFMI} is judged necessary for incorporating the mean stress effect accurately in design, irrespective of the design load model.

- If a railway bridge is designed to carry one train type, the mean stress can be incorporated directly via the R-ratios generated by the train passage on the bridge influence lines, and not via λ_{HFMI} expressions as these were derived using mixed traffic.
- It is well known that extreme peak stresses might affect the stability of HFMI-treated weldments in steel bridges. Statistical analyses are conducted to provide a base for the verification of HFMI-treated details with reference to this issue. The characteristic combination associated with the serviceability limit state check is found to be the best-studied choice to make this verification in composite road steel bridges.
- The thesis provides some practical recommendations for HFMI treatment if applied on existing bridges. This includes crack inspection and removal of paint layer prior to treatment, corrosion protection, sandblasting and light grinding to remove sharp groove edges after treatment, and some other recommendations such as the positioning of indentor or TIG electrode when the treatment is applied on cracked bridges.

4.2 Suggestion for future work

The work conducted in this thesis focuses on the effects of HFMI treatment in existing bridges, and the design considerations in HFMI-treated weldments in steel bridges. The following subjects are proposed for further research.

- In this thesis, fatigue endurance is calculated using strain-based fatigue and finite element removal. Calculation of fatigue life of existing structures treated via HFMI treatment is suggested via fracture mechanics calculations. This may enable a better understanding of the crack behaviour after HFMI treatment. Besides, welding simulation is encouraged to consider the distortions and residual stress into account. This might need verification with experimental results which were not possible in this work as all specimens have failed from the base metal.
- Despite that HFMI treatment emphasizes its capability in extending the life of cracked weldments, it is still recommended to apply it only on crack-free weldments. This is due to the inherent inaccuracy in crack detection. Therefore, it is encouraged to study the inaccuracy margin in different crack detection methods which can be used on bridges such as ultrasonic scanning. This would extend the field of application of HFMI treatment to cracked structures.
- The use of HFMI treatment should be studied for old steel types which were used for constructing bridges in the last decade.
- The study on the mean stress effect in road bridges includes more than 800k and 400k vehicles in Sweden and the Netherlands respectively. Investigating the road traffic from other countries in terms of mean stress effect and comparing the results to the proposed framework in this thesis contributes to further understanding and framework development and validation.
- Investigating more railway traffic from Sweden and other countries is required to further verify the proposed framework for the mean stress in railway bridges. Besides, a base of verification of peak stresses is needed in railway bridges using a similar statistical analysis presented in this work.
- The proposed design procedures given in this work can be extended to other fields of application where HFMI treatment can be used to increase the fatigue strength of steel weldments such as offshore structures and cranes. This requires realistic in-service stress assessment using real load.

References

[1] Pantura, "Needs for maintenance and refurbishment of bridges in urban environments," 2011.

[2] I. L. K. Reid, D. M. Milne, and R. E. Craig, *Steel Bridge Strengthening: a study of assessment and strengthening experience and identification of solutions*. Thomas Telford, 2001.

[3] B. Imam and M. Chryssanthopoulos, "A review of metallic bridge failure statistics," in *Bridge Maintenance, Safety and Management: Proceedings of the Fifth International IABMAS Conference*, pp. 3275–3282, 2010.

[4] H. Al-Karawi, A. Manai, and M. Al-Emrani, "A literature review for the state of the art,"

[5] P. Shams-Hakimi, F. Carlsson, M. Al-Emrani, and H. Al-Karawi, "Assessment of in-service stresses in steel bridges for high-frequency mechanical impact applications," *Engineering Structures*, vol. 241, p. 112498, 2021.

[6] R. M. Barker and J. A. Puckett, *Design of highway bridges based on AASHTO LRFD bridge design specifications*. 1987.

[7] F. M. Russo, D. R. Mertz, K. H. Frank, K. E. Wilson, *et al.*, "Design and evaluation of steel bridges for fatigue and fracture–reference manual," tech. rep., National Highway Institute (US), 2016.

[8] E. C. for Standardization, "Eurocode 3: Design of steel structures. part 1.9: Fatigue," 2003.

[9] A. Hobbacher *et al.*, *Recommendations for fatigue design of welded joints and components*. Springer, 2009.

[10] M. Al-Emrani and M. Aygül, "Fatigue design of steel and composite bridges," *Chalmers Reproservice*, 2014.

[11] Y. Yao, B. Ji, Z. Fu, J. Zhou, and Y. Wang, "Optimization of stop-hole parameters for cracks at diaphragm-to-rib weld in steel bridges," *Journal of Constructional Steel Research*, vol. 162, p. 105747, 2019.

[12] I. Takahashi, "A simple repair method of fatigue cracks using stop-holes reinforced with wedge members: applicability to reinitiated cracks and effects of an anti-fatigue smart paste," *Welding International*, vol. 34, no. 7-9, pp. 267–287, 2020.

[13] Z. Fu, Q. Wang, B. Ji, and Z. Yuanzhou, "Rewelding repair effects on fatigue cracks in steel bridge deck welds," *Journal of Performance of Constructed Facilities*, vol. 31, no. 6, p. 04017094, 2017.

[14] R. J. Dexter, J. M. Ocel, *et al.*, "Manual for repair and retrofit of fatigue cracks in steel bridges," tech. rep., United States. Federal Highway Administration, 2013.

[15] D. R. Mertz *et al.*, "Steel bridge design handbook: Redundancy," tech. rep., United States. Federal Highway Administration. Office of Bridges and Structures, 2015.

[16] A. Akyel, M. Kolstein, and F. Bijlaard, "Fatigue strength of repaired welded connections made of very high strength steels," *Engineering Structures*, vol. 161, pp. 28–40, 2018.

[17] P. Haagensen and S. Maddox, "IIW recommendations on post weld improvement of steel and aluminium," *IIW Doc*, vol. 13, pp. 1815–00, 2003.

[18] M. M. Pedersen, O. Ø. Mouritsen, M. R. Hansen, J. G. Andersen, and J. Wenderby, "Comparison of post-weld treatment of high-strength steel welded joints in medium cycle fatigue," *Welding in the World*, vol. 54, no. 7-8, pp. R208–R217, 2010.

[19] J. W. Fisher, A. W. Pense, R. E. Slockbower, and H. Hausammann, "Retrofitting fatigue damaged bridges," *Transportation Research Record*, no. 664, 1978.

[20] H. Al-Karawi, "Literature review on crack retrofitting in steel by tungsten inert gas remelting," *Ships and Offshore Structures*, pp. 1–6, 2022.

[21] J. C. Lippold, *Welding metallurgy and weldability*. John Wiley & Sons, 2014.

[22] Z. B. Gary Marquis, *IIW recomendations for the HFMI treatment for imporving the fatigue strength of welded joints*. Springer, 2016.

[23] J. Hedegård, M. Al-Emrani, M. Edgren, A. Manai, H. Al-Karawi, and Z. Barsoum, "Lifeext–prolonged life for existing steel bridges–livslängdsförlängning av befintliga stålbroar," 2020.

[24] L. Huo, D. Wang, and Y. Zhang, "Investigation of the fatigue behaviour of the welded joints treated by tig dressing and ultrasonic peening under variable-amplitude load," *International journal of Fatigue*, vol. 27, no. 1, pp. 95–101, 2005.

[25] K. Anami, C. Miki, H. Tani, and H. Yamamoto, "Improving fatigue strength of welded joints by hammer peening and TIG-dressing, structural eng./earthquake eng," JSCE, 2000.

[26] P. Haagensen, E. S. Statnikov, and L. Lopez-Martinez, "Introductory fatigue tests on welded joints in high strength steel and aluminium improved by various methods including ultrasonic impact treatment (UIT)," *IIW Doc*, vol. 13, pp. 1748–98, 1998.

[27] L. L. Martinez, A. Blom, H. Trogen, and T. Dahle, "Fatigue behaviour of steels with strength levels between 350 and 900 mpa influence of post weld treatment under spectrum loading," in *Proceeding of the North European Engineering and Science Conference,(NESCO), Welded High-Strength Steel Structures, Stockholm, Edited by AF Bloom, EMAS Publishing, London*, 1997.

[28] M. Leitner, M. Stoschka, and W. Eichlseder, "Fatigue enhancement of thin-walled, high-strength steel joints by high-frequency mechanical impact treatment," *Welding in the World*, vol. 58, no. 1, pp. 29–39, 2014.

[29] A. Abdullah, M. Malaki, and A. Eskandari, "Strength enhancement of the welded structures by ultrasonic peening," *Materials & Design*, vol. 38, pp. 7–18, 2012.

[30] T. Ishikawa, K. Yamada, T. Kakiichi, and H. Li, "Extending fatigue life of cracked out-of-plane gusset by ICR treatment," *Structural Engineering/Earthquake Engineering*, vol. 28, no. 1, pp. 21s–28s, 2011.

[31] H. Al-Karawi, M. Al-Emrani, and J. Hedegård, "Crack behaviour after high-frequency mechanical impact treatment in welded S355 structural steel," in *Bridge Maintenance, Safety, Management, Life-Cycle Sustainability and Innovations*, pp. 3113–3119, CRC Press, 2021.

[32] S. J. Maddox, M. Doré, and S. D. Smith, "A case study of the use of ultrasonic peening for upgrading a welded steel structure," *Welding in the World*, vol. 55, no. 9, pp. 56–67, 2011.

[33] M. Leitner and M. Stoschka, "Effect of load stress ratio on nominal and effective notch fatigue strength assessment of hfmi-treated high-strength steel cover plates," *International Journal of Fatigue*, vol. 139, p. 105784, 2020.

[34] E. Mikkola, M. Doré, and M. Khurshid, "Fatigue strength of HFMI treated structures under high R-ratio and variable amplitude loading," *Procedia Engineering*, vol. 66, pp. 161–170, 2013.

[35] H. Shimanuki, T. Mori, and M. Tanaka, "Study of a method for estimating the fatigue strength of welded joints improved by UIT," *IIW Doc. XIII*, vol. 2495, 2013.

[36] M. Tai and C. Miki, "Improvement effects of fatigue strength by burr grinding and hammer peening under variable amplitude loading," *Welding in the World*, vol. 56, no. 7, pp. 109–117, 2012.

[37] C. Miki and M. Tai, "Fatigue strength improvement of out-of-plane welded joints of steel girder under variable amplitude loading," *Welding in the World*, vol. 57, no. 6, pp. 823–840, 2013.

[38] T. Ummenhofer, S. Herion, J. Hrabowsky, S. Rack, I. Weich, G. Telljohann, S. Dannemeyer, H. Strohbach, H. Eslami-Chalandar, A. Kern, *et al.*, "Refresh–extension of the fatigue life of existing and new welded steel structures (lebensdauerverlängerung bestehender und neuer geschweißter stahlkonstruktionen)," *FOSTA Research Association for Steel Applications (Forschungsvereinigung Stahlanwendung e. Düsseldorf*, 2011.

[39] T. Deguchi, M. Mouri, J. Hara, D. Kano, T. Shimoda, F. Inamura, T. Fukuoka, and K. Koshio, "Fatigue strength improvement for ship structures by ultrasonic peening," *Journal of marine science and technology*, vol. 17, no. 3, pp. 360–369, 2012.

[40] T. Ishikawa, M. Shimizu, H. Tomo, H. Kawano, and K. Yamada, "Effect of compression overload on fatigue strength improved by ICR treatment," *International Journal of Steel Structures*, vol. 13, no. 1, pp. 175–181, 2013.

[41] T. Okawa, H. Shimanuki, Y. Funatsu, T. Nose, and Y. Sumi, "Effect of preload and stress ratio on fatigue strength of welded joints improved by ultrasonic impact treatment," *Welding in the World*, vol. 57, no. 2, pp. 235–241, 2013.

[42] H. Polezhayeva, D. Howarth, M. Kumar, B. Ahmad, and M. E. Fitzpatrick, "The effect of compressive fatigue loads on fatigue strength of non-load carrying specimens subjected to ultrasonic impact treatment," *Welding in the World*, vol. 59, no. 5, pp. 713–721, 2015.

[43] U. Kuhlmann, S. Breunig, T. Ummenhofer, and P. Weidner, "Entwicklung einer dast-richtlinie für höherfrequente hämmerverfahren: Zusammenfassung der durchgeführten untersuchungen und vorschlag eines dast-richtlinien-entwurfs," *Stahlbau*, vol. 87, no. 10, pp. 967–983, 2018.

[44] M. Al-Emrani and B. Akesson, *Steel structures Course Literature – VSM 191*. No. 321, 1989.

[45] V. Knysh, S. Solovei, V. Kir'yan, and V. Bulash, "Increasing the corrosion fatigue resistance of welded joints by high-frequency mechanical peening," *Strength of Materials*, vol. 50, no. 3, pp. 443–447, 2018.

[46] M. Leitner, Z. Barsoum, and F. Schäfers, "Crack propagation analysis and rehabilitation by HFMI of pre-fatigued welded structures," *Welding in the World*, vol. 60, no. 3, pp. 581–592, 2016.

[47] H. Al-Karawi, "Material and residual stress improvement in S355 welded structural steel using mechanical and thermal post-weld treatment methods," *Steel Construction*, vol. 15, no. 1, pp. 51–54, 2022.

[48] H. Al-Karawi, M. Al-Emrani, and R. Haghani, "Fatigue life estimation of treated welded attachments via high-frequency mechanical impact treatment (HFMI-treatment)," *Modern Trends in Research on Steel, Aluminium and Composite Structures*, p. 472, 2021.

[49] N. Powers, D. M. Frangopol, R. Al-Mahaidi, and C. Caprani, "Maintenance, safety, risk, management and life-cycle performance of bridges, melbourne, australia," *Proceedings of the Ninth International Conference on Bridge Maintenance, Safety and Management*, 2018.

[50] H.-P. Günther, U. Kuhlmann, and A. Dürr, "Rehabilitation of welded joints by ultrasonic impact treatment (UIT)," in *IABSE Symposium Report*, vol. 90, pp. 71–77, International Association for Bridge and Structural Engineering, 2005.

[51] K. Houjou, K. Takahashi, K. Ando, and H. Abe, "Effect of peening on the fatigue limit of welded structural steel with surface crack, and rendering the crack harmless," *International Journal of Structural Integrity*, vol. 5, no. 4, pp. 279–289, 2014.

[52] R. Fueki and K. Takahashi, "Prediction of fatigue limit improvement in needle peened welded joints containing crack-like defects," *International Journal of Structural Integrity*, vol. 9, no. 1, pp. 50–64, 2018.

[53] R. Fueki, K. Takahashi, and K. Houjou, "Fatigue limit prediction and estimation for the crack size rendered harmless by peening for welded joint containing a surface crack," *Materials Sciences and Applications*, vol. 6, no. 06, p. 500, 2015.

[54] C. Branco, V. Infante, and R. Baptista, "Fatigue behaviour of welded joints with cracks, repaired by hammer peening," *Fatigue & Fracture of Engineering Materials & Structures*, vol. 27, no. 9, pp. 785–798, 2004.

[55] S. J. Maddox, M. Doré, and S. D. Smith, "A case study of the use of ultrasonic peening for upgrading a welded steel structure," *Welding in the World*, vol. 55, no. 9-10, pp. 56–67, 2011.

[56] G. P. Tilly, P. A. Jackson, S. J. Maddox, and R. Henderson, "Fatigue strengthening of welds in light rail structures," in *Proceedings of the Institution of Civil Engineers-Bridge Engineering*, vol. 163, pp. 147–152, Thomas Telford Ltd, 2010.

[57] J. Fisher, H. Hausammann, and A. Pense, "Retrofitting procedures for fatigue damaged full scale welded bridge beams, final report, january 1979.," 1979.

[58] H. Zhang, D. Wang, L. Xia, Z. Lei, and Y. Li, "Effects of ultrasonic impact treatment on pre-fatigue loaded high-strength steel welded joints," *International Journal of Fatigue*, vol. 80, pp. 278–287, 2015.

[59] Y. Kudryavtsev, J. Kleiman, A. Lugovskoy, L. Lobanov, V. Knysh, O. Voitenko, and G. Prokopenko, "Rehabilitation and repair of welded elements and structures by ultrasonic peening," *Welding in the World*, vol. 51, no. 7-8, pp. 47–53, 2007.

[60] W. Fricke, "Guideline for the fatigue assessment by notch stress analysis for welded structures," *International Institute of Welding*, vol. 13, pp. 2240–08, 2008.

[61] H. C. Yildirim, G. B. Marquis, and Z. Barsoum, "Fatigue assessment of high-frequency mechanical impact (HFMI)-improved fillet welds by local approaches," *International Journal of Fatigue*, vol. 52, pp. 57–67, 2013.

[62] M. M. Pedersen, O. Ø. Mouritsen, M. R. Hansen, and J. G. Andersen, "Experience with the notch stress approach for fatigue assessment of welded joints," in *Swedish Conference on Light Weight Optimized Welded Structures, Borlänge*, 2010.

[63] N. E. Dowling, *Mechanical behavior of materials: engineering methods for deformation, fracture, and fatigue*. Pearson, 2012.

[64] E. S. Statnikov, V. Muktepavel, and A. Blomqvist, "Comparison of ultrasonic impact treatment (UIT) and other fatigue life improvement methods," *Welding in the World*, vol. 46, no. 3-4, pp. 20–32, 2002.

[65] R. Kogler *et al.*, "Steel bridge design handbook: Corrosion protection of steel bridges," tech. rep., United States. Federal Highway Administration. Office of Bridges and Structures, 2015.

[66] M. A. Wahab and M. Sakano, "Experimental study of corrosion fatigue behaviour of welded steel structures," *Journal of materials processing technology*, vol. 118, no. 1-3, pp. 116–121, 2001.

[67] S. Gkatzogiannis, J. Weinert, I. Engelhardt, P. Knoedel, and T. Ummenhofer, "Corrosion fatigue behaviour of HFMI-treated butt welds," *International Journal of Fatigue*, vol. 145, p. 106079, 2021.

[68] M. Daavari and S. S. Vanini, "Corrosion fatigue enhancement of welded steel pipes by ultrasonic impact treatment," *Materials Letters*, vol. 139, pp. 462–466, 2015.

[69] V. Knysh, S. Solovej, L. Nyrkova, L. Shitova, and A. Kadyshev, "Influence of corrosion damage on cyclic fatigue life of tee welded joints treated by high-frequency mechanical peening," *The Paton Welding J*, vol. 9, pp. 42–46, 2016.

[70] V. Knysh, S. Solovei, L. Nyrkova, I. Klochkov, and S. Motrunich, "Influence of the atmosphere corrosion on the fatigue life of welded t-joints treated by high frequency mechanical impact," *Procedia Structural Integrity*, vol. 16, pp. 73–80, 2019.

[71] B. Fereidooni, M. Morovvati, and S. Sadough-Vanini, "Influence of severe plastic deformation on fatigue life applied by ultrasonic peening in welded pipe 316 stainless steel joints in corrosive environment," *Ultrasonics*, vol. 88, pp. 137–147, 2018.

[72] J. Weinert, S. Gkatzogiannis, I. Engelhardt, P. Knödel, and T. Ummenhofer, "Increasing the fatigue strength of welded structural details in corrosive environments by applying high frequency mechanical impact treatment," *Welding and Cutting*, vol. 18, no. 6, 2019).

[73] Y. Fan, X. Zhao, and Y. Liu, "Research on fatigue behavior of the flash welded joint enhanced by ultrasonic peening treatment," *Materials & Design*, vol. 94, pp. 515–522, 2016.

[74] R. Govindaraj, R. Sudhakaran, K. Eazhil, S. Mahendran, and L. Senthilkumar, "Influence of high-frequency mechanical peening on the fatigue life of stainless steel joints in corrosive environment," *Transactions of the Indian Institute of Metals*, vol. 72, no. 12, pp. 3233–3239, 2019.

[75] M. Leitner, S. Gerstbrein, M. Ottersböck, and M. Stoschka, "Fatigue strength of HFMI-treated high-strength steel joints under constant and variable amplitude block loading," *Procedia Engineering*, vol. 101, pp. 251–258, 2015.

[76] P. Shams-Hakimi, *Fatigue improvement of steel bridges with high-frequency mechanical impact treatment*. PhD thesis, Chalmers Tekniska Hogskola (Sweden), 2020.

[77] J. Schubnell, E. Carl, M. Farajian, S. Gkatzogiannis, P. Knödel, T. Ummenhofer, R. Wimpory, and H. Eslami, "Residual stress relaxation in HFMI-treated fillet welds after single overload peaks," *Welding in the World*, vol. 64, no. 6, pp. 1107–1117, 2020.

[78] T. Yonezawa, H. Shimanuki, and T. Mori, "Relaxation behavior of compressive residual stress induced by uit under cyclic loading," *Q. J. Jpn. Weld. Soc*, vol. 37, pp. 44–51, 2019.

[79] E. Mikkola, H. Remes, and G. Marquis, "A finite element study on residual stress stability and fatigue damage in high-frequency mechanical impact (HFMI)-treated welded joint," *International Journal of Fatigue*, vol. 94, pp. 16–29, 2017.

[80] E. Mikkola and H. Remes, "Allowable stresses in high-frequency mechanical impact (HFMI)-treated joints subjected to variable amplitude loading," *Welding in the World*, vol. 61, no. 1, pp. 125–138, 2017.

[81] P. Shams-Hakimi, H. Al-Karawi, and M. Al-Emrani, "High-cycle variable amplitude fatigue experiments and design framework for bridge welds with high-frequency mechanical impact treatment," *Steel Construction*, 2022.

[82] J. Maljaars, "Evaluation of traffic load models for fatigue verification of european road bridges," *Engineering Structures*, vol. 225, p. 111326, 2020.

[83] J. Leander, "Kalibrering av säkerhetsfaktorer för tunga specialfordon på järnvägsbroar," 2022.

[84] E. C. for Standardization, "Eurocode 1: Actions on strucutres - part 2: Traffic loads on bridges," 2003.

[85] K. TRVINFRA-00227, "Bro och broliknande konstruktion, byggande," *Trafikverket infrastrukturregelverk*, 2020.

[86] S. S. Nazzal, E. Mikkola, and H. C. Yıldırım, "Fatigue damage of welded high-strength steel details improved by post-weld treatment subjected to critical cyclic loading conditions," *Engineering Structures*, vol. 237, p. 111928, 2021.

[87] J. Schubnell, E. Carl, M. Farajian, S. Gkatzogiannis, P. Knödel, T. Ummenhofer, R. Wimpory, and H. Eslami, "Correction to: Residual stress relaxation in HFMI-treated fillet welds after single overload peaks," *Welding in the World*, vol. 65, no. 11, pp. 2247–2247, 2021.

[88] P. Gerster, "Höherfrequente hämmerverfahren – vorstellung derneuen dast-richtlinie 026," 2019.

[89] F. Carlsson, *Modelling of traffic loads on bridges based on measurements of real traffic loads in Sweden*. PhD thesis, Lund University, 2006.

[90] T. Vrouwenvelder *et al.*, "The JCSS probabilistic model code," *Structural Safety*, vol. 19, no. 3, pp. 245–251, 1997.

[91] I. Vayas and A. Iliopoulos, *Design of steel-concrete composite bridges to Eurocodes*. CRC press, 2013.